Plant Physiology and Biochemistry 234 (2026) 111324

Contents lists available at ScienceDirect

Plant Physiology and Biochemistry

journal homepage: www.elsevier.com/locate/plaphy

Plant–microbiome interactions are associated with enhanced salinity tolerance and methane emissions in rice

Murat Aycan [a,*], Dorra Fakhet [b,1], Pedro J. Picazo [b,1], Seda Bodur [c,d], Hirohiko Nagano [c], Rasit Asiloglu [c], Iker Aranjuelo [b], Toshiaki Mitsui [a]

[a] Laboratory of Biochemistry, Institute for Social Innovation and Cooperation, Niigata University, Niigata, 950-2181, Japan
[b] Agrobiotechnology Institute (IdAB-CSIC), Consejo Superior de Investigaciones Científicas Gobierno de Navarra, Av. Pamplona 123, Mutilva Baja, 31006, Spain
[c] Institute of Science and Technology, Niigata University, Niigata, 950-2181, Japan
[d] Department of Horticulture, Faculty of Agriculture, Recep Tayyip Erdogan University, Rize, 53300, Türkiye

ARTICLE INFO

Keywords:
Salinity stress
Rhizosphere microbiome
Greenhouse gases
Methanogenic archaea
Gene expression
High-throughput sequencing
Stress physiology

ABSTRACT

Salinity is a severe environmental stressor that reduces crop performance, alters soil microbial communities, and influences greenhouse gas emissions such as methane (CH_4). Climate change is expected to further increase salinity globally. Although plants have evolved physiological and molecular mechanisms to cope with salinity, the role of plant–microbiome interactions in salinity tolerance and their link to CH_4 emissions remain poorly understood. Here, we investigated the interactions among plant salinity tolerance, rhizobiome, and CH_4 emission under salinity stress. We used salt-tolerant and salt-sensitive rice genotypes grown in nutrient-poor paddy field soil and nutrient-rich commercial nursery soil under climate-controlled greenhouse conditions with salinity stress until harvesting. Salt-sensitive genotypes exhibited decreases in early biomass and gas exchange due to salinity stress under nutrient-rich nursery soil. However, salinity effects were mitigated by plant–microbiome interactions, which improved plant growth performance. Rhizosphere microbiome analysis revealed that Rhizobacteria, including Cyanobacteria, were associated with plant development and salinity tolerance. Salinity altered methanogenic archaeal communities, especially Methanobacteria and Methanocellia, with salt-tolerant genotypes releasing more CH_4 during stress. Gas exchange and antioxidant enzyme activity were positively correlated with CH_4 emissions, suggesting an association between improved physiological performance under salinity and microbial methanogenesis. Gene expression profiling revealed a significant upregulation of hormone- and ion-transport-related genes in paddy soil, which may be associated with stress tolerance, microbial activity, and CH_4 emissions. This study proposes a mechanistic framework that links plant salinity tolerance, rhizosphere microbial dynamics, and methane production, illustrating how these interconnected processes shape plant performance and the environmental outcomes. These findings emphasize the necessity of balancing agricultural productivity with CH_4 emissions and soil resilience under climate-induced stress.

1. Introduction

The growing global population and rising environmental stressors, such as salinity, pose a threat to food sustainability. More than 20% of the global irrigated land is currently affected by soil salinization, and it is projected to be over 50% by 2050, particularly in coastal and arid regions (Singh, 2021). Salinity stress reduces plant development by causing ionic toxicity and osmotic imbalance, resulting in significant yield reductions. At the same time, the world's food demand is projected to increase by 70%, which means that grain production would need to rise by 50% to feed an estimated 9.7 billion people by the middle of the century (FAO, 2009). Therefore, it is crucial to develop methods that enhance crop resistance to salinity.

Rice is one of the salt-sensitive crops cultivated in over 100 countries and is a staple food for more than half of the global population, particularly in Asia (Fukagawa and Ziska, 2019). Due to the increasing

* Corresponding author. Laboratory of Biochemistry, Institute for Social Innovation and Cooperation, Niigata University, 8050 Ikarashi 2-no-cho, Nishi-ku, Niigata, Niigata City, 950-2181, Japan.
E-mail address: murataycan@agr.niigata-u.ac.jp (M. Aycan).
[1] These authors contributed equally.

https://doi.org/10.1016/j.plaphy.2026.111324
Received 14 January 2026; Received in revised form 21 April 2026; Accepted 24 April 2026
Available online 25 April 2026

effect of natural disasters and climate change (earthquakes, tsunamis, and sea-level rise-related salinity), more than 30% of paddy fields will be unusable by the end of the century (Genua-Olmedo et al., 2022). Especially, sea-level rise increases soil salinization and damages the coastal ecosystem, which is the main ecosystem for rice cultivation (Mazhar et al., 2022). Developing salt-tolerant genotypes using genetic engineering has made progress (Aycan et al., 2023; Rana et al., 2019). However, emerging evidence suggests that the root-associated microbiome–plant interactions also play an essential role in modulating plant responses to salt stress in rice (Ali et al., 2024).

The majority of root-associated microbiome resides in the rhizosphere soil, which plays a functional role in nutrient uptake, hormone signaling, and ion homeostasis for plants (Xun et al., 2024). Additionally, they support the promotion of plant growth and mitigate salinity stress (H. Li et al., 2021; Y. Wang et al., 2022) by maintaining ionic and osmotic balance and ensuring membrane stability (Gupta et al., 2023; Sahu et al., 2021). Plant varieties and soil salinity influence the structure of the microbial community in the rhizosphere. According to previous research, the structure of the rhizosphere microbiome in salt-tolerant plants differs from that in salt-sensitive plants (Lei et al., 2025; Zhang et al., 2024). Salt-tolerant genotypes can have specific microbial taxa, such as halotolerant plant growth–promoting rhizobacteria, including Bacillus, Halomonas, Pseudomonas, and Paenibacillus species, which may enhance crop adaptation under salt stress by improving physiological and biochemical stress responses, including ion homeostasis, antioxidant activity, and hormone regulation (AbuQamar et al., 2024; Gupta et al., 2023; Radhakrishnan and Krishnasamy, 2024; Sarkar et al., 2018). Also, rhizosphere microbial communities contribute to key soil processes such as carbon cycling through the decomposition of organic matter by heterotrophic bacteria and fungi (Henneron et al., 2020; Ling et al., 2022), nitrogen cycling through microbial nitrogen fixation and denitrification (Hao et al., 2022; Mosley et al., 2022; Zhao et al., 2023), and the regulation of greenhouse gas emissions, particularly nitrous oxide (N_2O), carbon dioxide (CO_2), and methane (CH_4) fluxes (Maier et al., 2022; Ortega et al., 2023).

CH_4 emissions are the primary concern of greenhouse gas emissions in paddy fields. Studies show that the global warming potential of CH_4 emissions is approximately 28 times greater than that of CO_2 emissions over a hundred years (IPCC, 2014; X. Wang et al., 2022). Flooded rice paddies are a significant source of CH_4 emissions worldwide, accounting for approximately 11% of all anthropogenic methane emissions. This is because fields remain flooded throughout the rice-growing season. (Lee et al., 2023; Yan et al., 2009). Methane is generated in the anaerobic microsites of soil by methanogenic archaea (e.g., Methanobacteria, Methanocellia, and Methanosarcina) and emitted into the atmosphere mostly via rice aerenchyma (Bao et al., 2014; Lee et al., 2014; Liesack, 2000). In the aerobic microsites of paddy fields, such as a part of rhizosphere soils near the rice root zone and surface water zone, methanotrophic bacteria (e.g., Methylobacter and Methylocystis) are active and oxidize the generated CH_4 before emitting it to the atmosphere. The structure and function of these methanogenic archaeal communities, as well as their interactions with methane-oxidizing bacteria, are significantly influenced by soil conditions, plant characteristics, and environmental stresses, including salinity (Fernández-Baca et al., 2021; Liu et al., 2022; Zhao et al., 2025). Soil salinity may alter CH_4 emissions through altering microbial community structure and metabolic activity. In non-vegetated aquatic systems, increasing salinity often suppresses methanogenesis and stimulates alternative pathways, such as sulfate reduction and aerobic respiration, which occur under salinity conditions (Soued et al., 2024). However, in vegetated environments such as paddy fields, the interactions between salinity, rhizosphere microbiome composition, and CH_4 emissions remain poorly understood, particularly across rice genotypes with differing salinity tolerance.

Here we aimed to determine (i) whether contrasting soil systems differing in microbial composition and nutrient status (using paddy field soil with its natural microbiome and commercial high-temperature sterilized granular nursery soil with its relatively nutrient-rich and lower microbiome diversity) influence rice plant tolerance to salt, (ii) if soil salinity affects methane production, and (iii) how rice plants' ability to tolerate salt (using a salt-tolerant and -sensitive rice genotype) affects methane production. Our results provide new insights into the impact of interactions between plants and microbes on rice growth, microbiome structure, and methane emissions under salinity stress, all of which are crucial for environmental sustainability in high-salt environments.

2. Materials and methods

2.1. Plant and soil material

The plant material *Oryza sativa* ssp. *Japonica* genotypes YNU31–2–4 and YNU31–2–4–SL were used as the salt-tolerant (ST) and salt-sensitive (SS) rice genotypes, respectively. The ST and SS genotypes exhibit only two single-nucleotide polymorphisms (SNPs) while remaining similar in genome sequencing (Aycan et al., 2023; Aycan and Mitsui, 2026). The nutrient-poor paddy field-derived soil (PS) samples were collected from five different locations (0-20 cm depth) of a paddy field in Kashiwazaki, Niigata, Japan (37°22′40.8″ N 138°36′35.5″ E). The collected soil samples were well mixed, and physicochemical characteristics were determined (27 mg/kg of N, 37 mg/kg of P, 74 mg/kg of K, 0.2–0.3 dS/m of EC, and 5.68 pH). The nutrient-rich nursery culture soil (NS) was obtained commercially, which is high-temperature-sterilized granular soil (Honen Agri Co., Ltd., Honens soil No. 1) (460 mg/kg of N, 460 mg/kg of P, 460 mg/kg of K, 0.03–0.05 dS/m of EC, and 4.5–5.5 pH). High-temperature-sterilized soil was used as a low-microbial-diversity control to establish a reproducible baseline for evaluating microbiome effects under controlled conditions. Heat sterilization is widely applied in plant–microbiome experiments because it effectively reduces microbial load while maintaining soil structure and nutrient composition within an acceptable range (Li et al., 2023). It should be noted that NS and PS differ not only in microbial diversity but also in nutrient availability and other soil characteristics; therefore, this experimental design does not allow complete separation of microbiome effects from soil physicochemical influences and instead reflects their combined impact. Although alternative sterilization methods exist, the objective here was to establish a consistent low-diversity reference condition for evaluating microbiome presence versus reduced-microbiome conditions; therefore, the use of heat-sterilized soil followed by targeted microbial inoculation provided a practical and controlled experimental framework. Accordingly, plant responses observed in this study should be interpreted as resulting from integrated soil–plant–microbiome interactions rather than solely microbiome-associated effects.

2.2. Experimental design

The seeds of ST and SS genotypes were de-husked and soaked for 2 weeks at 4 °C under dark conditions. Soaked seeds were transferred to a 32-well seedling tray filled with rice nursery culture soil under a controlled growth chamber with light-dark cycles of 26/23 °C, 12 h of light (350 μmol m^{-2} s^{-1}) and 12 h of darkness, and 70% relative humidity for 10 days. After seven days, the seedlings were transferred to ambient conditions in a greenhouse for an additional ten days for climate adaptation. Healthy and uniform-looking seventeen-day-old seedlings were transferred to 2-liter plastic pots (15.5 cm diameter × 12 cm depth × 20 cm height) filled with NS or PS and placed in a plastic water pool (65 L: 615 mm length × 350 mm width × 300 mm height) to simulate field conditions in a controlled greenhouse at 26/23 °C, 70% humidity, and ambient light conditions. The ST and SS genotypes cultivated in NS or PS soils were subjected to either 0 (control) or 75 mM NaCl (salinity) from 27 days after germination (DAG27) until harvesting, thereby capturing integrated physiological, microbiome, and methane emissions responses across the full growth period under

controlled conditions. A 75 mM NaCl concentration was used as a moderate salinity level commonly used in rice physiological studies, sufficient to induce measurable stress responses without causing severe growth inhibition or plant mortality (Aycan et al., 2023; Aycan and Mitsui, 2024; Koc et al., 2024; Nahar et al., 2023), while allowing microbial activity to be maintained. The experiment employed five biological replicates per treatment for growth and physiological measurements. Among these, three plants with uniform phenotypes were selected as biological replicates for biochemical, gene expression, and microbiome analysis. Plants of the same genotype (SS or ST) and soil type (NS and PS) were cultivated in the same pool in different pots to minimize microbial contamination between genotypes, soils, and treatments (Fig. S1). Plant leaf samples were collected 30 days after exposure to salt stress, where apparent morphological differences were observed (Aycan et al., 2024; Aycan and Mitsui, 2024), rapidly frozen in liquid nitrogen, and stored at −80 °C until further biochemical and gene expression-related experimental processing.

2.3. Leaf gas exchange measurements

The net photosynthetic rate (A_n, CO_2 m^{-2} s^{-1}), stomatal conductance (g_s, mol H_2O m^{-2} s^{-1}), transpiration rate (E, mmol H_2O m^{-2} s^{-1}), intercellular CO_2 concentration (C_i, μmol CO_2 m^{-2} s^{-1}), and the ratio of intercellular-to-ambient CO_2 concentration (C_i/C_a) were measured as leaf gas exchange parameters by using a portable photosynthesis LI-6400XL system (LI-6400-20, LI-COR Biosciences, Lincoln, NE, USA) from flag leaves at the flowering stage. The instantaneous water use efficiency (WUE_i) was calculated as the ratio of the net photosynthetic rate to the transpiration rate (A_n/E). The measurements were recorded from 9:00 to 15:00 h under clear sky (sunny) conditions with a photosynthetically active radiation (PAR) value above 1000 μmol m^{-2} s^{-1} to ensure maximum values, and the CO_2 concentration was maintained at 400 μmol s^{-1} in the chamber. The relative humidity ranged between 45% and 55%, and the leaf temperature was maintained at 26 °C.

2.4. Methane emissions measurement

Methane (CH_4) soil emissions from pot soil were quantified using the closed chamber method after 30 days of salinity stress (Minamikawa et al., 2015). A closed-top acrylic cylinder chamber with a volume of 6.8 L (16 cm diameter × 34 cm height) was placed over the pot to cover it without disturbing the soil and rice plant. Those pots were placed in the water pool (300 mm height), thus allowing the chambers to maintain the seal during the flux measurement. As the chambers have brims on their top and bottom, we stacked chambers when we found that the plant height was higher than a single chamber. By inserting a ring-shaped silicon rubber plate between two chambers, the sealing of the chambers was maintained.

We conducted monitoring of CH_4 concentration during the chamber covering gas volume to the pot using a real-time gas analyzer (LI-7810, Li-Cor, USA), following the protocol by Tokida (2021) and Kajiura and Tokida (2021). Briefly, the real-time gas analyzer recorded CH_4 concentrations (ppm) inside the chambers at a 1.0 s resolution for 10 min. The chamber and the gas analyzer were connected with tubing. The air inside the chamber was pumped and circulated between the chamber and the analyzer at a rate of 0.25 L/min by a pump built into the analyzer. In order to prevent the analyzer from potential condensation, a silica-gel dehumidification unit (Tokida, 2021) was connected in between the chamber and the gas analyzer inlet.

The dehumidification unit consisted of a Teflon tube placed in a cold-water bath that effectively condensed and removed moisture from the sampled air before entering the analyzer, preventing water interference in CH_4 signal detection. The unit consisted of a sealed container filled with moisture-absorbing silica gel through which the sampled air passed before entering the analyzer. This setup ensured stable CH_4 readings and protected the optical system from water vapor accumulation.

The LI-7810 measurements were performed first to observe real-time CH_4 concentration dynamics and evaluate emissions trends under different soil and salinity conditions. These results were later complemented by an independent gas chromatographic (GC) analysis for precise quantification of CH_4 fluxes.

For GC analysis, gas samples inside the chambers were collected at 0, 5 and 10 min after chamber closure using a syringe through a Suba Seal septum fixed in the chamber. 30 mL of gas were taken from each chamber, stored at overpressure in pre-evacuated 20 mL glass vials, and analyzed using a gas chromatograph (GC-2014, Shimadzu Corporation, Kyoto, Japan) equipped with a stainless packed column (GC-2014-SUS-3.0 × 2m-Active Carbon-60/80-JK, GL Sciences, Tokyo, Japan) and a flame ionizer detector for CH_4 detection; samples were injected utilizing a headspace auto-sampler (2000H, HTA S.R.L., Brescia, Italy). Standards of CH_4 (0.62, 4.87, 8.12, and 9.74 ppm) were analyzed simultaneously with the samples.

CH_4 emissions fluxes were calculated as the change in gas concentration over 10 min. Fluxes were expressed as mg CH_4 m^{-2} h^{-1}. The air temperature in a greenhouse was used to convert gas volume to weight in the gas equation of state. Here, the air pressure inside the chambers was assumed to be equal to that of the ambient air. Cumulative emissions during the evaluated period were estimated using the trapezoidal rule of integration, as described by Minamikawa et al. (2015) and Lasar et al. (2025). Chambers were removed after each gas sample was taken.

2.5. Plant growth, physiological, and harvesting determination

To observe plant salinity tolerance differences between soil types (NS and PS) during the growth period, plant height, chlorophyll content (SPAD), and normalized vegetation index (NDVI) values were collected weekly from 0 weeks (DAG27, salt stress application day) to 8 weeks (DAG83, flowering). The plant heights were measured using a ruler. The chlorophyll content was recorded using an SPAD-502Plus meter (Konica Minolta, Tokyo, Japan). The NDVI values were collected using a GreenSeeker sensor (Trimble Agriculture, Trimble Inc., Westminster, CO, USA).

After harvesting, the main agronomic traits, such as plant height (PH), root length (RL), plant biomass (PB), root biomass (RB), tiller number (TN), panicle number (PN), panicle length (PL), spikelet number (SN), 1000-grain weight (TGW), grain number per panicle (GNPP), and yield per plant (YPP), were determined.

2.6. Biochemical analysis

The malondialdehyde (MDA) measurement was performed utilizing a revised method established by Dhindsa and Matowe (1981). The 0.5 g leaf sample was homogenized with 5 ml of a 0.1% trichloroacetic acid solution. The mixture was subsequently centrifuged at 12500×g and 25 °C for 20 min. A volume of 2 ml of the supernatant was mixed with 2 ml of thiobarbituric acid-trichloroacetic acid (TCA) solution. The mixture was incubated for 30 min at 90 °C, after which the reaction was terminated by placing the tube in a cold bath for 10 min. The chromogen generated was quantified at wavelengths of 520 and 600 nm using a double-beam spectrophotometer (U-2900, Hitachi, Tokyo, Japan).

The hydrogen peroxide (H_2O_2) concentration was recorded by the Loreto and Velikova (2001) method with slight modifications. A frozen leaf sample weighing 0.3 g underwent homogenization with 3 mL of a 1% (w/v) trichloroacetic acid (TCA) solution. The homogenate was subjected to centrifugation at 10,000×g and 4 °C for 10 min. The liquid component was subsequently mixed with 0.75 ml of a 10 mM K-phosphate buffer solution at pH 7.0 and 1.5 ml of a 1 M KI solution. The concentration of H_2O_2 was determined by comparing the absorbance of the supernatant at 390 nm with a standard calibration curve. The concentration of H_2O_2 was ascertained using a standard curve established within the range of 10–1000 μmol ml^{-1}. Hydrogen peroxide (H_2O_2) was measured in micromoles per gram of fresh weight (μmol g^{-1} FW).

The osmoprotectant, free proline (PRO) concentration, was determined using the methodology of Bates et al. (1973) with minor adjustments. The snap-frozen leaf sample (0.5 g) was homogenized using 3% sulfosalicylic acid solution (10 mL). The homogenate was incubated for 24 h at 4 °C under dark conditions. The incubated homogenate was centrifuged at 10,000×*g* for 5 min at 25 °C. The supernatant (1 mL) obtained was combined with ninhydrin (1 mL) and glacial acetic acid (1 mL) in a glass test tube. The mixture was subjected to a high temperature (100 °C) for 1 h in a hot bath. After heat treatment, the tubes were immersed in an ice bath for 20 min. Toluene (2 mL) was added to the tube and incubated for 30 min to extract proline. The toluene phase was extracted from the tube, and the absorbance was measured at a wavelength of 520 nm using a double-beam spectrophotometer U-2900 (Hitachi, Tokyo, Japan).

One gram of frozen leaf powder samples was homogenized with 4 mL of 1 M phosphate buffer (pH 7.0) and 0.1 mM Na-EDTA (10 mL). The homogenate was subjected to centrifugation at 15,000×*g* for 15 min at 4 °C. The liquid above the sediment, referred to as the supernatant, was used to evaluate antioxidant enzyme activity, as described by Tejera García et al. (2004).

The evaluation of superoxide dismutase (SOD) activity was performed by measuring its capacity to inhibit the photochemical reduction of nitro blue tetrazolium (NBT), utilizing the methodology established by Cakmak and Marschner (1992). The unit of superoxide dismutase (SOD) is defined as the amount of enzyme required to achieve a 50% decrease in the activity of nitroblue tetrazolium (NBT) at 25 °C. The SOD was measured and expressed as units per minute per gram of fresh weight. The absorbance measurement was performed at a wavelength of 650 nm using a double-beam spectrophotometer (U-2900, Hitachi, Tokyo, Japan).

The assessment of catalase (CAT) activity involved observing the rate of decline in absorbance at a wavelength of 240 nm over 3 min following the degradation of hydrogen peroxide (H_2O_2) (Aebi, 1984). The experimental configuration involved the combination of 0.8 mL of a phosphate buffer solution with a concentration of 50 mM and a pH of 7.6, which also contained 0.1 mM Na-EDTA. Furthermore, 0.1 mL of a 100 mM H_2O_2 solution and 0.1 mL of enzyme extract were combined to obtain a total volume of 2 mL.

The activity of ascorbate peroxidase (APX) was assessed by measuring the reduction in absorbance at 290 nm over 1 min, in accordance with the methodology outlined by Amako et al. (1994). The assay solution comprised 100 μL of extract sample, 50 mM potassium phosphate buffer at pH 7.6, 0.5 mM H_2O_2, and 0.1 mM ascorbate. The reaction commenced with the addition of the enzyme extract, and the reduction in absorbance was documented.

2.7. Na^+ and K^+ ion measurements

The sodium (Na^+) and potassium (K^+) ion concentrations in the leaves and roots of rice plants were measured after harvesting using a wet digestion method described by Pequerul et al. (1993) and analyzed by "Polarized Zeeman atomic absorption spectrophotometry" (Z-6100, Hitachi, Tokyo, Japan).

2.8. Real-time quantitative PCR analysis

Total RNA was extracted from 30-day-old salt-exposed plant leaves using the TRIzol method (Simms et al., 1993). RNA integrity was determined using gel electrophoresis, while RNA concentration was quantified using a NanoDrop™ One^C spectrophotometer (Thermo Fisher Scientific, Waltham, MA, USA). The total RNA samples were reverse transcribed into cDNA using the ReverTra Ace qPCR RT Mix with gDNA Remover kit (Toyobo, Osaka, Japan). RT-PCR amplification was conducted in a 10 μl reaction mixture, which included 1 μl of cDNA, 3.6 μl of ddH_2O, 0.2 μl each of 10 pmol sense (forward) and antisense (reverse) primers, and 5 μl of SsoFast.

EvaGreen Supermix (Bio-Rad Laboratories). PCR was conducted in triplicate for each gene: 98 °C for 2 min, 98 °C for 2 s, 60 °C for 5 s, and 75 to 95 °C for 10 s for the melting curve (39 cycles). Real-time PCR was performed using the CFX96 Real-time PCR Detection System (Bio-Rad Laboratories, Hercules, CA, USA). The mean of three separate plant samples was used for all real-time PCR assays. The normalization of gene expression for the target gene (Table S1) was calculated using the $2^{-\Delta\Delta CT}$ method as described by Livak and Schmittgen (2001) employing reference gene *OsACTIN1* (Os03g0718100).

2.9. Microbial and bioinformatics analysis

Soil samples were collected from the rhizosphere of three pots with three biological replicates per genotype (ST and SS) grown under control and salinity treatments in both soil types (NS and PS). Each pot contained a single plant, and the rhizosphere soil was carefully collected 30 days after salt stress exposure. According to the manufacturer's instructions, total microbiome DNA was extracted from 0.5 g of the rhizosphere soil sample using ISOIL for Bead Beating (Nippon Gene, Tokyo, Japan). The V4 region of the 16S rRNA gene in the extracted DNA was amplified using the 515F/806R universal primers (Abellan-Schneyder et al., 2021; Amaral-Zettler et al., 2009), tailed with Illumina barcoded adapters (San Diego, CA, USA) (Caporaso et al., 2012). Primary polymerase chain reaction (PCR), purification, index PCR (Nextera XT Index Kit v2 SetA, Illumina Inc., San Diego, CA, USA), and Illumina MiSeq sequencing (MiSeq Kit V2 300 cycles, 2 × 300 paired-end reads on an Illumina MiSeq sequencing platform, Illumina Inc., San Diego, CA, USA) were performed, as described previously (Asiloglu et al., 2024). All of the raw sequence data obtained in this study have been deposited in the NCBI database under the BioProject ID PRJNA1446220.

Raw data (FastQ) were analyzed using the QIIME2 pipeline (version 2023.9, available at https://qiime2.org/). Error correction, quality filtering, adaptor, doubleton, and chimera removal were performed using DADA2 (Callahan et al., 2016) with reads truncated at 200 bp for each paired-end read, corresponding to a quality score >30, and allowing forward and reverse sequences to overlap >50 bp. QIIME2's q2-feature-classifier plugin was used against the most recent bacterial SILVA Ribosomal RNA database (138.2) (Quast et al., 2012) for the taxonomy assignment of the bacteria (Burki et al., 2020; Yilmaz et al., 2014). Prior to denoising, sequence quality was assessed using the demux summarize function in QIIME2 to determine trimming and truncation parameters (Bolyen et al., 2019). Microbial community composition was visualized using taxa bar plots. Specific taxa, including methanogenic groups such as Methanobacteria, were filtered and analyzed to assess their contribution to methane (CH_4) emissions. Pearson correlation analysis was performed to evaluate the relationships between selected microbial taxa, gene expression levels, and CH_4 emissions. Correlation coefficients (r) and significance levels (p-values) were calculated using R software, with statistical significance set at $P < 0.05$.

2.10. Statistical analysis

The plant data were evaluated by using analysis of variance (ANOVA) to determine the impact of genotype (G), soil (S), treatment (T), GxS, GxT, and GxSxT interactions. The differences were determined using Tukey's honestly significant difference (HSD) test at a significance threshold of $P < 0.05$. This analysis was conducted using RStudio software employing the 'glht' function inside the 'multcomp' package (Hothorn et al., 2008; Kassambara and Mundt, 2016). Principal component analysis (PCA) was conducted using the 'factoextra' and

'FactoMineR' packages to elucidate the differentiation across genotypes and soil based on physiological, biochemical, post-harvesting, and yield-related data under control and salinity stress conditions (Kassambara and Mundt, 2016; Lê et al., 2008). Euclidean distance matrices were calculated to evaluate similarities, and the findings were shown alongside the PCA graph. The data was subjected to hierarchical clustering using the heatmap function in the 'pheatmap' package in the RStudio program (Kolde, 2010). The random forest classification and variable importance analysis were conducted using the 'randomForest' package in the RStudio program (Breiman, 2001) to evaluate the relative contribution of the rhizosphere microorganisms in differentiating plant growth and salinity tolerance and methane emissions under salt stress conditions. Pearson correlation analysis was performed to evaluate the relationships between CH_4 emissions, gene expression levels, and selected microbial taxa. Correlation coefficients (r) and significance levels (*P*-values) were calculated using R software. As the analysis focused on a limited number of selected variables, multiple comparison correction was not applied due to the hypothesis-driven selection of a limited number of variables, and statistical significance was set at $P < 0.05$.

3. Results

3.1. Paddy soil improves plant growth and photosynthesis

To investigate the effect of the rhizosphere microbiome (including bacterial and archaeal communities) on salinity tolerance, ST and SS genotypes, which are grown in NS and PS, were exposed to salt stress from DAG 27 until harvesting. Salinity significantly reduced plant growth from week 1 (W1) in the SS genotype, but it was reduced from W6 in NS (Fig. 1A and B). Interestingly, salinity did not significantly reduce plant growth in either ST and SS genotypes grown in PS, although PS contains significantly lower nutrients compared to NS (Fig. 1C and D). At the same time, we observed higher SPAD values in ST and SS genotypes grown in NS and PS under salinity conditions. However, after two months of salinity, most of the ST and SS plants showed similar

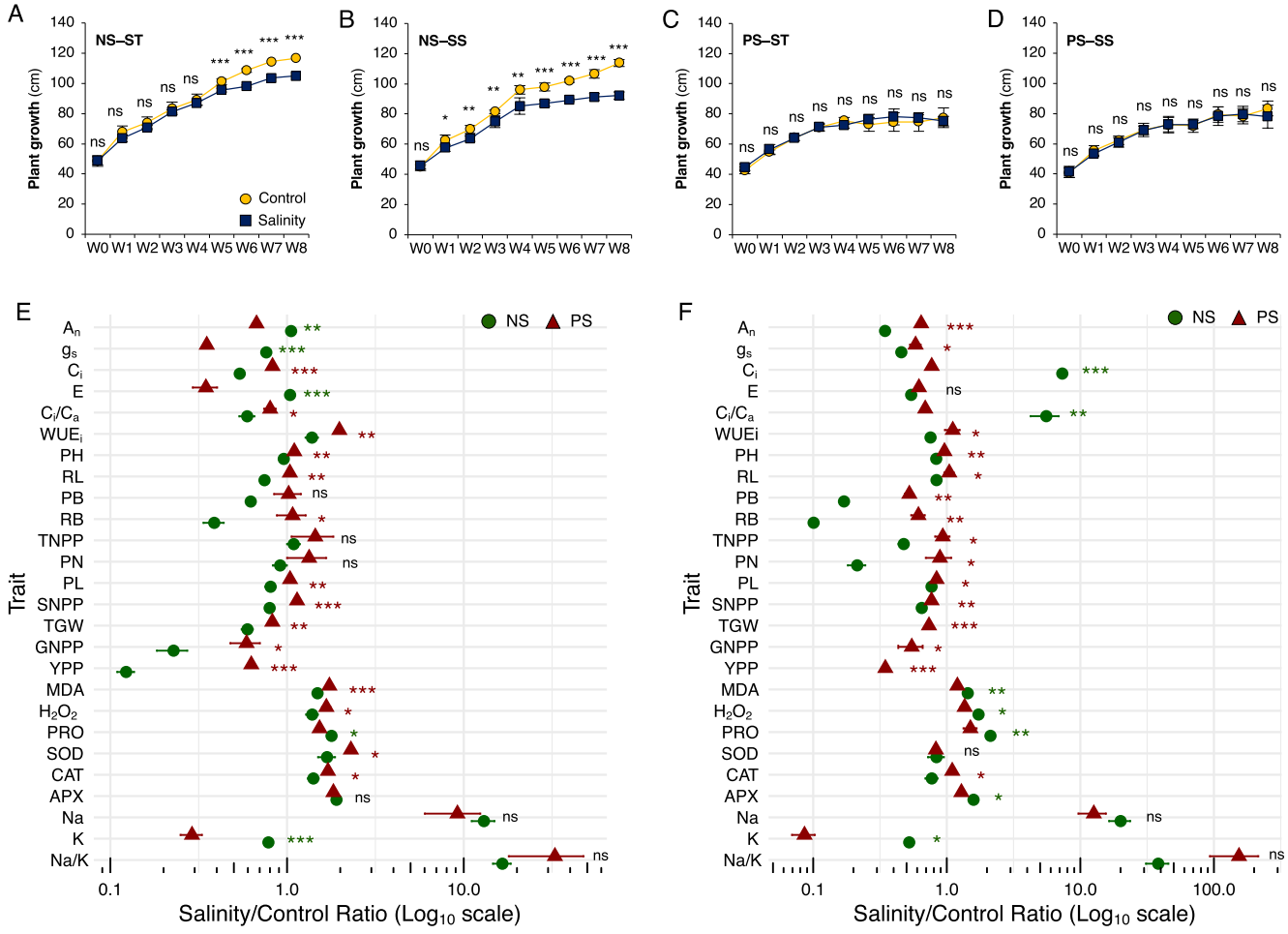

Fig. 1. Phenotypic responses of salt-tolerant (ST) and salt-sensitive (SS) rice genotypes to salinity under nursery soil (NS) and paddy soil (PS) conditions. **(A)** Plant growth performance of NS-ST, **(B)** NS-SS, **(C)** PS-ST, and **(D)** PS-SS plants under control (yellow color) and salinity (blue color) treatments for 8 weeks. **(E)** Log_{10}-transformed response ratios (salinity/control) for physiological and agronomic traits in ST and **(F)** SS rice genotypes grown under NS (green circle) and PS (red triangle) conditions. Data represent mean ± SD (n = 3–5). Asterisks indicate statistically significant differences between salt and control conditions at each time point and NS and PS for each genotype (*$P< 0.05$, **$P< 0.01$, ***$P < 0.001$; *Student's t-test*). Abbreviations: A_n, net photosynthetic rate; APX, ascorbate peroxidase; CAT, catalase; CH_4, methane C_i, intercellular CO_2 concentration; C_i/C_a, intercellular to ambient CO_2 concentration ratio; E, transpiration rate; GNPP, grain number per panicle; g_s, stomatal conductance; H_2O_2, hydrogen peroxide; K, K^+ concentration; MDA, malondialdehyde; Na, Na^+ concentration; NaK, Na^+/K^+ ratio; PB, plant biomass; PH, plant height; PL, panicle length; SNPP, spikelet number per panicle; PRO, proline content; PN, panicle number; RB, root biomass; RL, root length; SOD, superoxide dismutase; TGW, 1000-grain weight; TNPP, tiller number per panicle; WUEi, instantaneous water use efficiency; YPP, yield per plant.

SPAD values under both control and salinity conditions, except for the NS–ST treatment (Fig. S2A–S2D). During the same period, salinity did not significantly reduce NDVI values in the ST genotype until W8, but it significantly reduced NDVI in the SS genotype grown in NS from W5 (Fig. S2E and S2F). A similar pattern was observed in PS–ST and PS–SS (Fig. S2G and S2H).

Salinity significantly reduced the net photosynthesis rate (*An*) by −65% and −35% in SS genotypes grown in NS and PS, respectively. Salinity did not significantly affect the *An* in the NS–ST; however, it is reduced by −30% in the PS–ST (Fig. S2I). Interestingly, the *An* was significantly higher in ST (30%) and SS (430%) genotypes that grown in PS compared to NS. Also, the $\log_{10}$ (salinity/control) ratio was found to be considerably higher in the NS–SS (Fig. 1E and F, and S2I). The salinity significantly lowered stomatal conductance (g_s) and transpiration rate (E) in ST and SS genotypes grown in NS and PS. However, g_s and E were observed to be significantly higher in PS-ST and PS-SS, a similar pattern to that of *An* (Fig. S2J and S2K). Upon examining the $\log_{10}$ (salinity/control) ratio, g_s revealed a higher ratio in the SS–PS, but it was higher in the NS–ST. In the case of E, a significantly higher ratio of the NS–ST (Fig. 1E and F, Table 1).

The intercellular CO_2 concentration (C_i) and intercellular to ambient CO_2 concentration ratio (C_i/C_a) showed a similar pattern. Salinity significantly reduced C_i and the C_i/C_a ratio in NS–ST, PS-ST, and PS-SS. Interestingly, they were significantly increased in NS-SS. When we compared the soil type, PS showed significantly higher C_i, and the C_i/C_a ratio was almost the same in all genotypes and treatments except PS–SS (Fig. S2L and S2M). The $\log_{10}$ (salinity/control) ratios of C_i were observed to be higher in PS for the ST genotype and NS for the SS genotype; the C_i/C_a ratio was found to be higher in PS for the ST genotype, but it was higher in NS for the SS genotype (Fig. 1E and F). The instantaneous water use efficiency (WUE_i) was significantly increased in NS–ST and PS–ST but only decreased considerably in NS–SS. Additionally, WUE_i was significantly reduced in PS for all ST and SS genotypes compared to NS. The $\log_{10}$ (salinity/control) ratios of WUE_i were found to be significantly higher in PS for ST and SS genotypes (Fig. 1E and F, and S2N).

Table 1
ANOVA analysis of genotype (G), soil (S), treatment (T), and interaction effects on measured traits. Asterisks indicate significant differences (***$P<$ 0.001, **$P<$ 0.01, *$P<$ 0.05, ns = non-significant).

Traits	G	S	T	GxS	GxT	SxT	GxSxT
A_n	***	***	***	***	***	***	**
g_s	ns	***	***	***	***	***	***
E	***	***	***	ns	***	***	***
C_i	***	***	ns	*	***	***	***
C_i/C_a	ns	***	ns	ns	***	***	***
WUE_i	***	***	***	***	***	***	***
PH	**	***	***	***	***	***	*
RL	***	ns	***	***	**	***	**
PB	***	***	***	**	***	***	***
RB	***	***	***	***	***	***	**
TNPP	***	***	***	***	***	***	***
PN	ns	***	***	***	***	***	***
PL	ns	***	***	***	**	***	**
SNPP	ns	***	***	***	***	***	**
TGW	***	***	***	***	***	***	***
GNPP	***	**	***	***	***	***	ns
YPP	***	***	***	*	***	***	***
MDA	***	***	***	ns	**	***	***
H_2O_2	***	***	***	***	***	***	***
PRO	***	***	***	***	***	**	*
SOD	***	***	***	**	***	***	***
CAT	***	***	***	***	***	***	***
APX	***	***	***	**	***	***	***
Na	***	***	***	***	***	***	***
K	***	***	***	***	***	***	***
Na/K	***	***	***	***	***	***	***
CH_4	***	***	***	***	***	ns	ns
OsbHLH056	**	***	***	**	ns	***	ns
OsGRAS23	**	***	***	**	***	***	***
OsCKX2	ns	***	**	**	***	ns	***
OsABA1	ns	***	***	ns	***	***	***
OsIAA1	*	***	***	***	ns	***	****
OsHKT1	*	ns	**	***	***	***	ns
OsACO1	***	*	***	***	**	*	***
OsAKT1	***	ns	***	ns	***	ns	ns

Abbreviations: An, net photosynthetic rate; Gs, stomatal conductance; Ci, intercellular CO_2 concentration; E, transpiration rate; Ci/Ca, ratio of intercellular to ambient CO_2 concentration; WUEi, intrinsic water use efficiency; PH, plant height; RL, root length; PB, plant biomass; RB, root biomass; TNPP, tiller number per plant; PN, panicle number; PL, panicle length; SNPP, spikelet number per panicle; TGW, thousand-grain weight; GNPP, grain number per panicle; YPP, yield per plant; MDA, malondialdehyde; H_2O_2, hydrogen peroxide; PRO, proline; SOD, superoxide dismutase; CAT, catalase; APX, ascorbate peroxidase; Na, sodium content; K, potassium content; NaK, Na^+/K^+ ratio.

3.2. Paddy soil reduces ROS and enhances antioxidant enzyme activity

PS and NS showed different effects on the salinity tolerance capacity of ST and SS genotypes. Salinity significantly increased malondialdehyde (MDA) levels in ST and SS genotypes grown in NS and PS. However, PS significantly decreased the MDA level in all genotypes and conditions (Fig. 1E and F, and S3A). A similar pattern was observed in hydrogen peroxide (H_2O_2) production. Although salinity significantly increased H_2O_2 production in all genotypes and soil types, PS showed lower H_2O_2 production compared to NS in all genotypes and conditions (Fig. 1E and F, and S3B). Proline (PRO) accumulation significantly increased in ST and SS genotypes under salinity for all soil types. Proline accumulation was consistently higher in PS than NS across all genotypes and treatments (Fig. 1E and F, and S3C). Superoxide dismutase (SOD) activity was decreased in the NS–SS and PS–SS under salinity; however, ST genotypes showed increased SOD activity in both NS and PS soil types under salinity. Interestingly, PS showed significantly higher SOD activity in all genotypes and conditions under NS (Fig. 1E and F, and S3D). The catalase (CAT) activity significantly increased in ST genotypes grown in NS and PS soils under salinity conditions. The salinity reduced SOD activity in SS genotypes under NS soil type, but the CAT activity increased in SS genotypes in PS soil type under salinity conditions. The PS significantly increased SOD activity in all genotypes and conditions compared to the NS soil type (Fig. 1E and F, and S3E). The salinity significantly increased APX activity in both ST and SS genotypes grown in NS and PS soil types. However, proline accumulation was consistently higher in PS than NS across all genotypes and treatments (Fig. 1E and F, and S3F).

3.3. Paddy soil improves the post-harvest and yield-related traits under salinity conditions

After long-term exposure to salinity stress, both ST and SS plants exhibited significantly reduced plant height (PH) and root length (RL) under salinity across NS and PS soil types. PS exhibited a significantly lower PH compared to the NS soil type. A similar pattern was observed in RL. However, a significant difference was recorded in plant biomass (PB) and root biomass (RB) traits. Salinity significantly reduced PB and RB in both NS–ST and NS–SS, but not in PS–SS, which was not significantly affected. These results suggest that the ST genotype, particularly under PS conditions, exhibits greater resilience to salinity stress in terms of biomass retention (Fig. 1E and F, and S4).

The post-harvest traits of ST and SS genotypes grown in NS and PS soils were significantly reduced by salinity stress. Under salinity stress, the ST genotype exhibited higher tiller number per panicle (TNPP), panicle number (PN), panicle length (PL), and spikelet number per panicle (SNPP) compared to the SS genotype in NS and PS soil types. In contrast, the SS genotype exhibited pronounced reductions in all traits. The PS–ST and PS–SS genotypes were not significantly affected by salinity in terms of TNPP and PN. However, panicle length was reduced in the SS genotype by the effect of salinity on PL and SNPP traits. These

results demonstrate that the ST genotype retains superior yield-related performance under salinity stress, mainly when grown in nursery soil (Fig. 1E and F, and S5).

Although there were panicles and spikelets, the NS–SS genotype did not produce seeds under salinity stress conditions. Salinity significantly affects yield-related traits: 100-grain weight (TGW), grain number per panicle (GNPP), and yield per plant (YPP) were reduced by −40, −77, and −87% in the ST genotype grown in the NS type. The SS genotype grown in PS produces seeds under salt stress conditions. Even PS–ST and PS–SS were negatively affected by salinity stress; the reduction of TGW, GNPP, and YPP was significantly lower compared to the NS soil type. The data indicate that soil type has a significant influence on salinity stress responses, with paddy soil providing a more buffered environment that facilitates partial reproductive success in salt-sensitive genotypes (Fig. 1E and F, and S6).

The accumulation of Na^+ and K^+ ions showed significant differences among soil types, genotypes, and treatments. Under control conditions, Na^+ accumulation did not significantly change among genotypes and soil types. However, SS genotypes showed higher Na^+ accumulation compared to ST genotypes under salt stress conditions. Notably, the accumulated amount of Na^+ ions was higher in the NS soil than in the PS soil (Fig. S7A). On the other hand, K^+ accumulation decreased significantly under salinity stress. The most significant reduction of K^+ ions was observed in SS plants grown in NS soil (Fig. S7B). Therefore, the Na^+/K^+ ratio increased in NS–SS plants, indicating a significant ionic imbalance. The PS–ST and PS–SS genotypes exhibited lower Na^+/K^+ ratios under salinity stress (Fig. S7C), suggesting that paddy soil is better at maintaining ion balance than the nursery soil. These results indicate

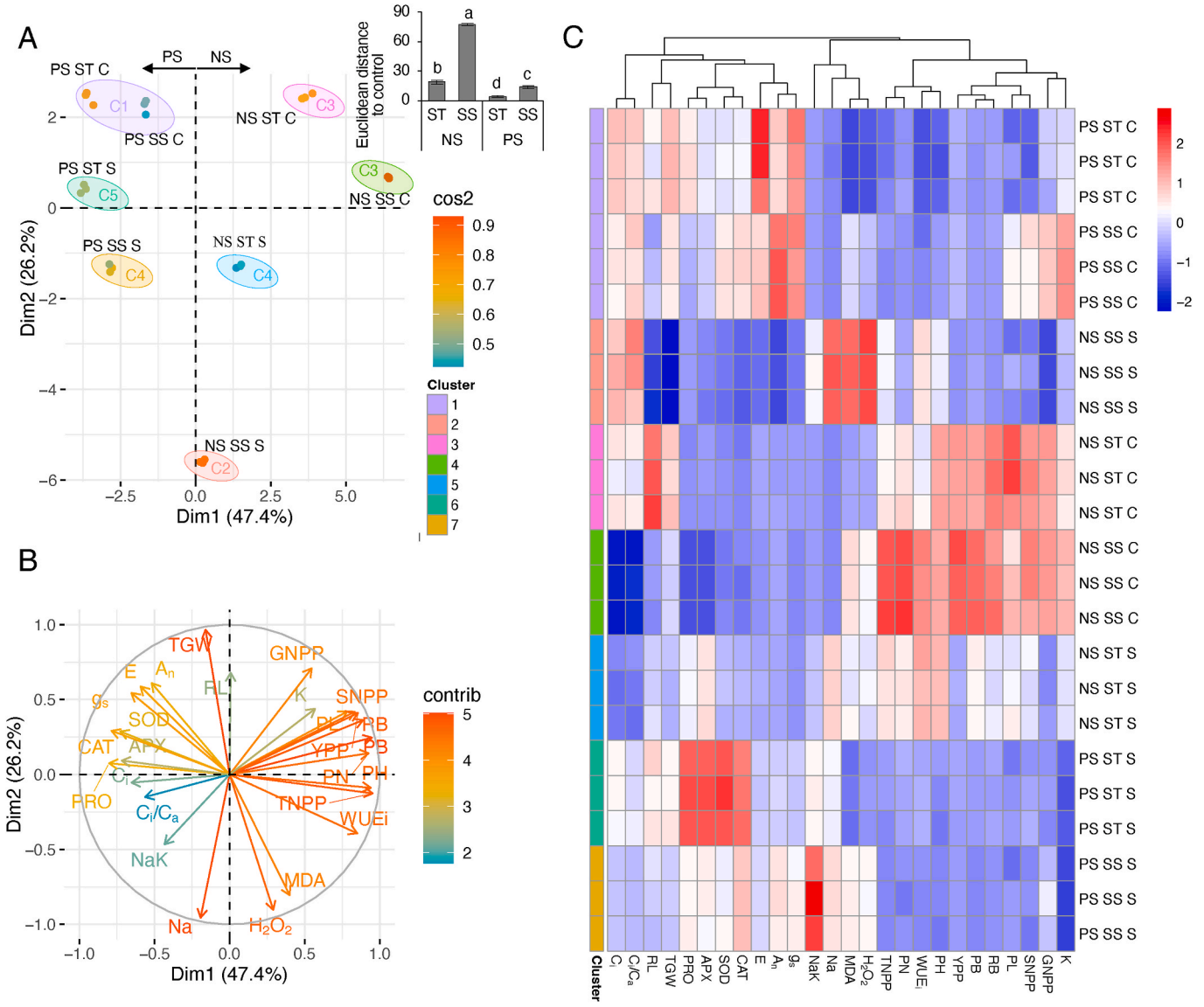

Fig. 2. Multivariate and correlation-based analysis of physiological and biochemical traits in salt-tolerant (ST) and salt-sensitive (SS) rice genotypes under salinity stress across nursery soil (NS) and paddy soil (PS) types. **(A)** Principal Component Analysis (PCA) based on measured physiological and biochemical parameters. Each point represents an individual sample, and ellipses indicate K-means clustering. **(B)** PCA biplot. **(C)** Heatmap of standardized (z-score) physiological and biochemical trait values across all samples. Rows represent treatments (grouped by genotype, soil, and salinity), and columns represent individual traits. Red indicates above-average values, while blue indicates below-average values. Left colors represent *K*-means clustering. Abbreviations: An, net photosynthetic rate; Gs, stomatal conductance; Ci, intercellular CO_2 concentration; E, transpiration rate; Ci/Ca, ratio of intercellular to ambient CO_2 concentration; WUEi, intrinsic water use efficiency; PH, plant height; RL, root length; PB, plant biomass; RB, root biomass; TNPP, tiller number per plant; PN, panicle number; PL, panicle length; SNPP, spikelet number per panicle; TGW, thousand-grain weight; GNPP, grain number per panicle; YPP, yield per plant; MDA, malondialdehyde; H_2O_2, hydrogen peroxide; PRO, proline; SOD, superoxide dismutase; CAT, catalase; APX, ascorbate peroxidase; Na, sodium content; K, potassium content; NaK, Na^+/K^+ ratio.

that soil type has a significant impact on the accumulation of ions from plants under salinity conditions (Fig. 2).

3.4. Rhizobacteria richness is associated with plant growth and tolerance

The number of amplicon sequence variants (ASVs) showed that the soil type, rice genotype, and salinity treatments changed the alpha diversity. Results showed that PS had a 289% higher total ASVs count (5854) than NS (1504). The ST genotype (4261) harbored approximately 11% more ASVs than the SS genotype (3773). The ASVs count of the control (4240) conditions was roughly 11% higher than the salinity (3792) conditions. The findings demonstrated that soil type, rice genotype, and salinity treatment significantly changed the alpha diversity, with the ST genotype grown in PS providing a more favorable environment for microbial diversity (Fig. 3A). Venn diagram analysis further revealed that the NS–ST genotype had higher unique ASVs under control (35%) and salinity conditions (25%), following the NS–SS genotype under salinity (18%) and control conditions (13%). The common ASVs among NS soil, rice genotypes, and conditions were observed at a frequency of around 1-2%. However, ST (25% of control and 14% of salinity) and SS (16% of control and 22% of salinity) showed almost similar amounts of unique ASVs in PS (Fig. 3B).

Based on 16S rRNA gene sequencing and taxonomic classification analysis, we identified the top 10 bacterial phyla that dominated each soil type, genotype, and treatment at the phylum level. Salinity stress altered the relative abundance of major bacterial taxa, including Actinobacteria, Bacteroidota, Bacilli, and Cyanobacteria (Fig. 3C). Random Forest analysis indicated that the high importance of Actinobacteria, Cyanobacteria, Bacteroidota, and Bacilli was significantly correlated with microbial community divergence across genotypes, soil types, and treatments (Fig. 3D and E). Additionally, cyanobacteria abundance and plant growth showed a significant positive correlation ($R = 0.41$, $P = 0.046$) in the Pearson correlation analysis (Fig. 3F). However, Actinobacteria, Bacteroidia, and Bacilli exhibited weak or no significant correlations with growth ($R = 0.35$, 0.018, and 0.14, respectively; $P > 0.05$; Fig. 3G–I). These results showed that Cyanobacteria may be positively associated with enhanced growth in rice under saline conditions, while the other taxa showed limited relevance under the tested conditions.

3.5. Salinity stress increases methane emissions

To validate methane (CH_4) emissions consistency, we first performed real-time monitoring using an Li-7810 analyzer to record CH_4 accumulation dynamics during chamber closure (Fig. 4A). The real-time CH_4 emissions (ppm) showed that the PS–ST salinity plants had the steepest slope, indicating fast and persistent release of methane during measurement. The NS–ST salinity showed a significant increase, but the SS genotypes in both soils displayed minimal differences in accumulation across treatments (Fig. 4A).

In parallel, we measured changes in CH_4 concentration from chamber-collected gas samples to confirm linear increases during enclosure (Fig. S8). CH_4 emissions pattern was significantly affected by rice genotype, soil type, and salinity treatment. In the nursery soil (NS) type, the ST genotype exhibited significantly elevated CH_4 emissions under salinity stress relative to the control (Fig. S8A). Nonetheless, the SS genotype exhibited no significant difference in CH_4 emissions between control and salinity stress conditions (Fig. S8B). In paddy soil (PS), the ST genotype displayed a solid and consistent CH_4 release, and salinity increased the CH_4 emissions (Fig. S8C). The SS genotype exhibited a delayed CH_4 emissions response, with remaining similar emissions between control and salinity stress (Fig. S8D).

These results demonstrate stable CH_4 accumulation (mg m^{-2} h^{-1}) across all treatments, supporting the reliability of subsequent flux calculations (Fig. 4B). The comprehensive CH_4 flux analysis indicated that PS–ST genotypes exhibited the highest flux, whereas salinity stress significantly elevated CH_4 flux compared to control conditions. The lowest CH_4 flow was observed in NS–SS control plants. Among all soil types, salinity stress tended to increase CH_4 emissions in ST genotypes more than in SS genotypes (Fig. 4B). A similar pattern was observed in real-time CH_4 accumulation curves. The overall CH_4 emissions patterns obtained from real-time monitoring (Fig. 4A) and GC-based flux measurements (Fig. 4B) were consistent, supporting the reliability of the observed treatment effects.

The Pearson correlation matrix analysis revealed a complex network of correlations between CH_4 emissions and plant physiological and biochemical characteristics. The flow of methane exhibited a notable positive correlation with metabolic traits, including PRO, SOD, CAT, and APX. Moderate positive correlations were identified among *gs*, E, and TGW, indicating that enhanced gas exchange capacity, increased TGW, and elevated biochemical activity (including PRO accumulation and heightened SOD, CAT, and APX activities) may be associated with methane release under salinity stress (Fig. 4C).

3.6. Methanogenic archaeal community structure and contribution to methane emissions under salinity stress conditions

To better understand the microbial causes of changes in CH_4 emissions patterns among rice genotypes, soil types, and salinity treatments, we examined the archaeal community. The archaeal community was influenced by salinity treatments, soil types, and rice genotypes. Methanosarcina, Bathyarchaeia, and Nitrososphaeria were identified as the three most prevalent archaeal groups across all treatments (Fig. 5A). When we extracted only the methanogenic archaeal community, the dominant groups were Methanosarcina, Methanomicrobia, Methanobacteria, and Methanococci. However, their proportional contributions varied depending on the genotype and soil type. Under salinity stress, the percentage of putative methanogenic taxa was generally higher, especially in paddy soil. On the other hand, methanogenic and non-methanogenic archaea were more evenly distributed in the nursery soil (Fig. 5B). According to random forest analysis, the most significant taxa for treatment classification were Methanomicrobia, Methanobacteria, Methanocellia, and Methanosarcina (Fig. 5C and D).

Pearson correlation analysis revealed that Methanomicrobia ($R = 0.12$, $P = 0.58$) and Methanosarcina ($R = 0.12$, $P = 0.56$) were not significantly correlated with CH_4 emissions. However, CH_4 emissions were significantly correlated with Methanobacteria ($R = 0.48$, $P = 0.019$) and Methanocellia ($R = 0.47$, $P = 0.02$) (Fig. 5E–H). These findings suggest that Methanobacteria and Methanocellia are strongly associated with methane emissions in rice systems, with other archaeal groups having minimal contributions to the dynamics of emissions under salinity stress.

3.7. Gene expression responses and their association with methane emissions

RT-qPCR analysis revealed significant transcriptional reprogramming of stress- and hormone-related genes in response to salinity stress, and soil type had a significant effect on expression patterns. Gene expression was significantly higher in PS compared with NS, indicating that conditions in PS mitigated the adverse effects of salinity on gene activity in both ST and SS genotypes (Fig. S9). Genes involved in hormonal signaling (*OsABA1*, *OsCKX2*, *OsIAA1*), ion transport (*OsHKT1*, *OsAKT1*), and transcriptional regulation (*OsbHLH056*, *OsGRAS23*) had higher expression levels in paddy soil. On the other hand, the ethylene biosynthetic gene *OsACO1* was differentially regulated depending on genotype. In the SS genotype, most genes were significantly downregulated in the high-salinity nursery soil but remained at stable expression levels or were even upregulated in paddy soil (Fig. 6A and B). This may explain the partial preservation of reproductive success observed in this soil type.

Correlation analysis further demonstrated that the expression of numerous genes was significantly correlated with methane emissions

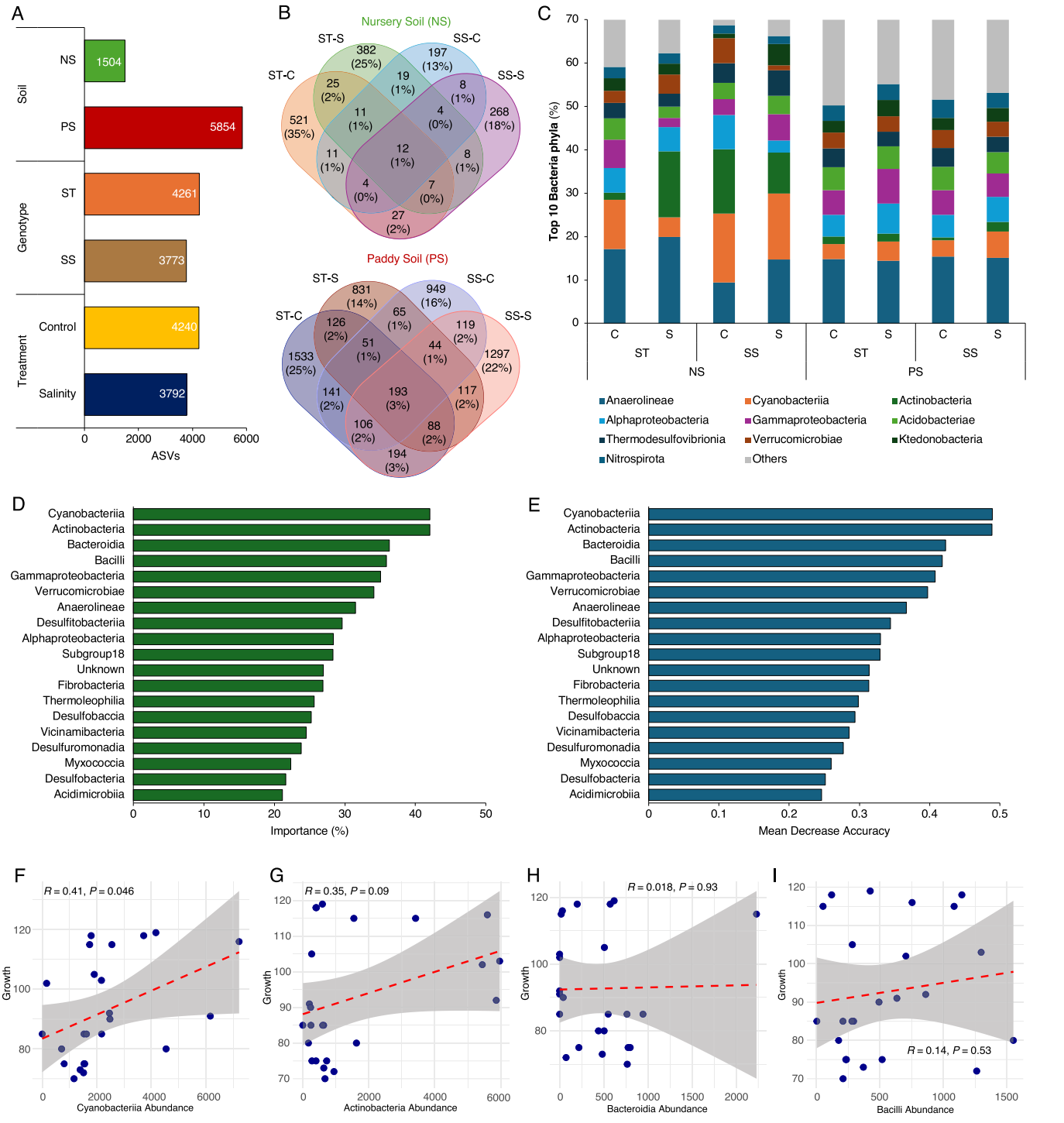

Fig. 3. Effects of soil type, genotype, and salinity treatment on bacterial community structure and indicator taxa in rice. **(A)** Bar plots showing the number of unique ASVs (Amplicon Sequence Variants) detected across different soil types [nursery soil, NS, green color, and paddy soil, PS, red color], genotypes [salt-tolerant (ST), orange color, and salt-sensitive (SS), brown color], and treatments [control (C), yellow color, and salinity (S), blue color]. **(B)** Venn diagrams representing shared and unique ASVs across genotypes (ST/SS) and treatments (S/C)—nursery soil (NS) upper panel, paddy soil (PS) lower panel. **(C)** Stacked bar plots displaying the percentage of the top 10 bacterial phyla across treatments and conditions [ST and SS genotypes in NS and PS soils under control (C) and salinity (S) treatments]. **(D)** Random Forest analysis identifying bacterial taxa most important for classifying samples. **(E)** Random Forest plot showing mean decrease in accuracy for each bacterial taxon, indicating its contribution to treatment classification. Scatter plots show Pearson correlations between methane flux (y-axis) and the relative abundance of **(F)** Cyanobacteria, **(G)** Actinobacteria, **(H)** Bacteroidia, and **(I)** Bacilli. Each point represents a treatment replicate. The red dashed lines indicate linear regression trends, and the shaded grey areas represent 95% confidence intervals. Each color corresponds to a specific taxon: Anaerolineae (dark blue), Cyanobacteriia (orange), Actinobacteria (green), Alphaproteobacteria (light blue), Gammaproteobacteria (purple), Acidobacteriae (light green), Thermodesulfovibrionia (dark navy), Verrucomicrobiae (brown), Ktedonobacteria (dark green), Nitrospirota (grey-blue), and Others (light grey).

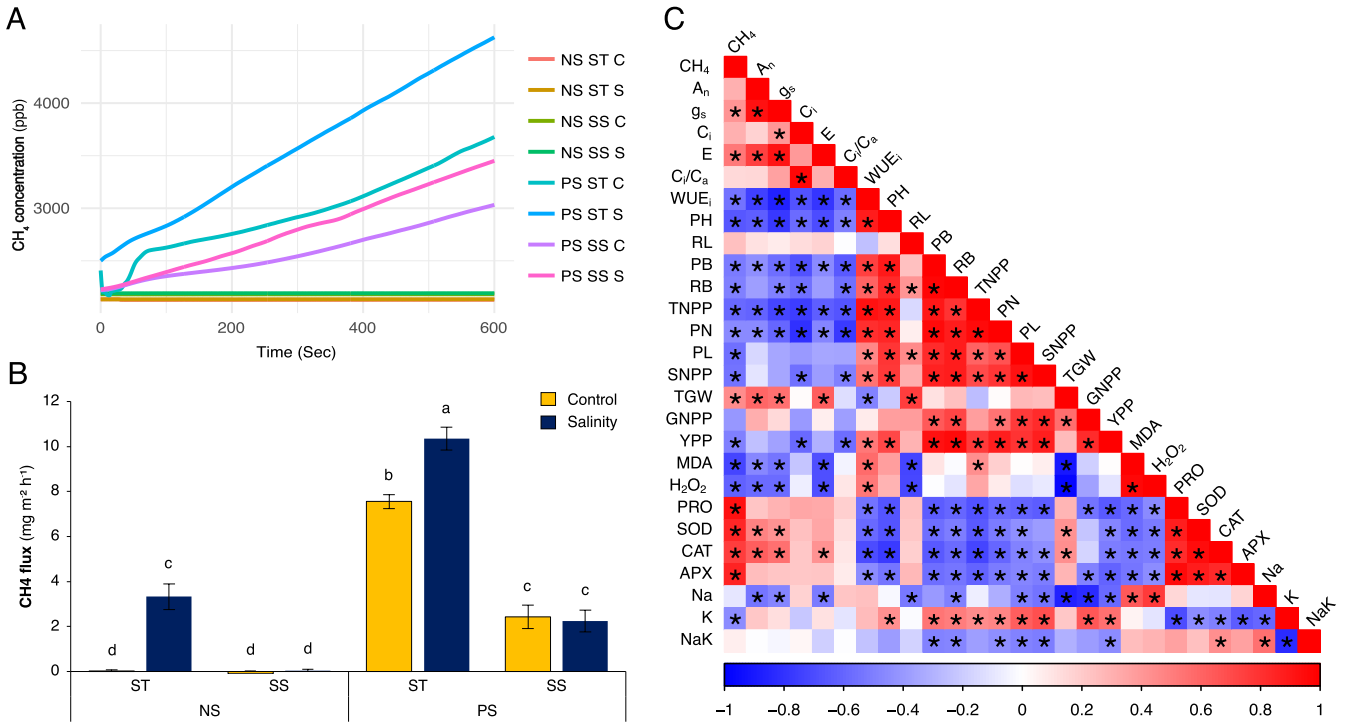

Fig. 4. Methane (CH_4) emission dynamics in salt-tolerant (ST) and salt-sensitive (SS) rice genotypes under control and salinity stress conditions in nursery soil (NS) and paddy soil (PS) types. **(A)** Real-time CH_4 concentration (ppm) curves over the measurement period for each treatment group [NS ST C (salmon), NS ST S (dijon), NS SS C (olive), NS SS S (jungle), PS ST C (turkish), PS ST S (azure), PS SS C (orchid), and PS SS S (magenta)]. **(B)** Total GS-based CH_4 flux (mg m^{-2} h^{-1}) calculated for each genotype (ST and SS)–soil (NS and PS)–treatment [Control (yellow) and salinity (blue)] combination. **(C)** Pairwise Pearson correlation matrix among all measured traits. Blue and red squares represent positive and negative correlations, respectively. The color intensity and square size correspond to the strength of the correlation coefficient (r). Statistically significant correlations are indicated. The values represent the means ± SDs (n = 3). Bars labeled with the same letter are not significantly different (Tukey's test, $P < 0.005$). Asterisks indicate statistically significant differences. Abbreviations: A_n, net photosynthetic rate; APX, ascorbate peroxidase; CAT, catalase; CH_4, methane C_i, intercellular CO_2 concentration; C_i/C_a, intercellular to ambient CO_2 concentration ratio; E, transpiration rate; GNPP, grain number per panicle; g_s, stomatal conductance; H_2O_2, hydrogen peroxide; K, K^+ concentration; MDA, malondialdehyde; Na, Na^+ concentration; NaK, Na^+/K^+ ratio; PB, plant biomass; PH, plant height; PL, panicle length; SNPP, spikelet number per panicle; PRO, proline content; PN, panicle number; RB, root biomass; RL, root length; SOD, superoxide dismutase; TGW, 1000-grain weight; TNPP, tiller number per panicle; WUEi, instantaneous water use efficiency; YPP, yield per plant.

(Fig. 6C). The relative gene expression of *OsABA1*, *OsIAA1*, and *OsAKT1* showed significant positive correlations with CH_4 emissions. Our results suggest that hormonal and ion homeostasis responses induced by salinity may be indirectly associated with methanogenesis under salinity conditions. On the other hand, genes such as *OsbHLH056* and *OsCKX2* exhibited a negative correlation with CH_4 emission, suggesting that their activation may be associated with stress adaptation processes that alter plant carbon allocation or root-microbe interactions, thereby reducing substrate availability for methanogenic archaea in the rhizosphere. We utilized Partial Least Squares Regression (PLSR) to integrate plant transcriptional regulation with the microbial community changes, employing gene expression and microbial taxa as predictors. The six-component optimized model explained roughly 60–70% of the total variation in CH_4 emissions (Fig. 6D), indicating that methane release is a trait influenced by both plant and microbial processes. Variable importance (VIP) scores in the projection identified *OsbHLH056*, in addition to bacterial groups (Cyanobacteria and Actinobacteria) and methanogenic archaeal groups (Methanomicrobia, Methanobacteria, and Methanococci), as primary predictors of methane efflux (Fig. 6E).

This comprehensive analysis demonstrates that plant transcriptional responses are associated with a physiological environment that may support enhanced bacterial and methanogenic activity in the rhizosphere by maintaining stress signaling, hormone balance, and ion homeostasis. The results indicated that ST in PS exhibited more positive gene expression profiles in response to salinity stress. This regulation aligns with the observed the microbial community changes that may contribute to CH_4 production. The connection between plant stress signaling and microbial methanogenesis may explain that specific genotypes and soil types that are associated with growth and yield under saline conditions also produce higher methane emissions.

4. Discussion

Salinity tolerance is not solely determined by internal physiological mechanisms; it is also strongly influenced by the composition and structure of associated microbial communities (Flowers and Colmer, 2008; Garbeva et al., 2008; Xavier et al., 2024). Plants employ a range of physiological and molecular strategies to mitigate the detrimental effects of salinity stress (Munns and Tester, 2008). The effectiveness of these strategies—such as enhanced photosynthesis, antioxidant activity, increased antioxidant capacity, reduced reactive oxygen species (ROS) production, limited accumulation of toxic Na^+ ions, and transcriptome adjustments—broadly defines a plant's ability to tolerate salinity (Aycan and Mitsui, 2024; Munns and Tester, 2008). However, the role of plant–microbiome interactions and their secondary metabolites, including processes like methanogenesis, remains underexplored in the context of salinity tolerance in rice.

To evaluate the impact of soil environment, including microbiome composition, on salinity tolerance and productivity, we focused on yield performance in two rice genotypes with contrasting salt tolerance: a salt-tolerant (ST) and a salt-sensitive (SS) genotype (Aycan et al., 2023). Under salinity stress, plants grown in the nutrient-poor paddy soil (PS)

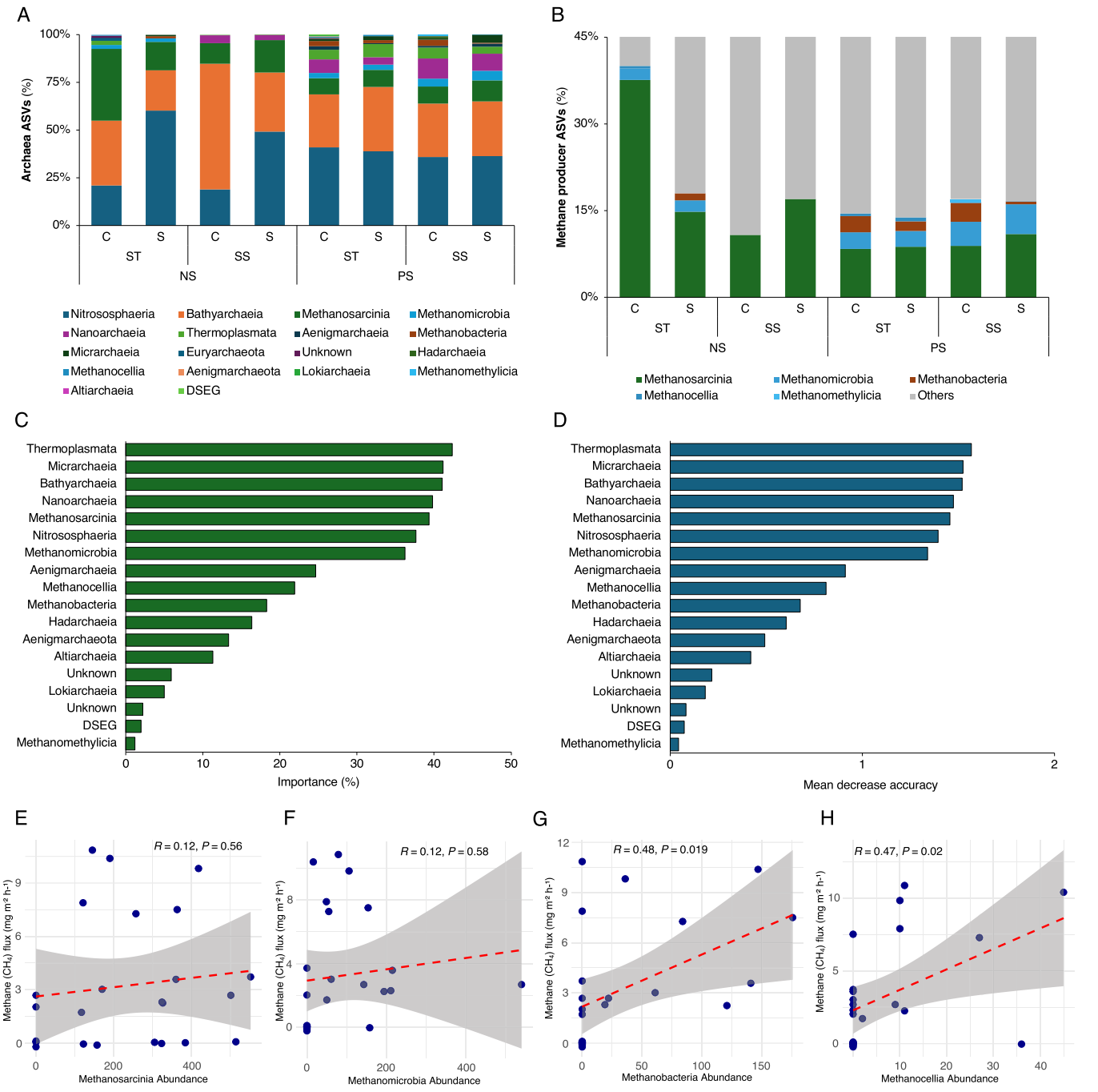

Fig. 5. Methanogenic archaeal community structure and its association with methane emissions under salinity and soil-type treatments. **(A)** Stacked bar plot showing relative abundance (%) of archaeal genera across all treatments (S; salinity, C; control, ST; salt-tolerant, SS; salt-sensitive, NS; nursery soil, PS; paddy soil). **(B)** Relative abundance of putative methanogenic archaeal taxa (colored) versus non-methanogenic taxa (grey) across treatments. **(C)** Random Forest analysis identifying archaeal taxa most important for classifying samples. **(D)** Random Forest plot showing mean decrease in accuracy for each methanogenic taxon, indicating its contribution to treatment classification. Scatter plots show Pearson correlations between methane flux (y-axis) and the relative abundance of **(E)** Methanosarcina, **(F)** Methanomicrobia, **(G)** Methanobacteria, and **(H)** Methanocellia. Each point represents a treatment replicate. The red dashed lines indicate linear regression trends, and the shaded grey areas represent 95% confidence intervals. For panel A, each color corresponds to a specific archaeal taxon: Nitrososphaeria (dark blue), Bathyarchaeia (orange), Methanosarcinia (green), Methanomicrobia (purple), Nanoarchaeia (light blue), Thermoplasmata (grey), Aenigmatarchaeia (black), Methanobacteria (brown), Micrarchaeia (light green), Euryarchaeota (dark navy), Unknown (pink), Hadarchaeia (dark green), Methanocellia (teal), Aenigmarchaeota (red), Lokiarchaeia (olive green), Methanomethylia (cyan), Altiarchaeia (blue-green), and DSPEG (light mint green). For panel B, each color corresponds to a specific archaeal group: Methanosarcinia (green), Methanomicrobia (blue), Methanobacteria (brown), *Methanocellia* (light blue), Methanomethylia (dark blue), and Others (grey).

achieved significantly higher grain yield compared to those grown in nutrient-rich nursery soil (NS). Although salinity reduced crop yield per plant across all treatments, these reductions were markedly less severe in PS than in NS. Notably, SS genotypes grown in PS were able to produce seeds under salinity, whereas NS-grown SS plants failed to produce grain despite PS's relatively lower nutrient content. These improvements in yield performance were accompanied by enhanced physiological responses in PS-grown plants. Under salinity stress, rice

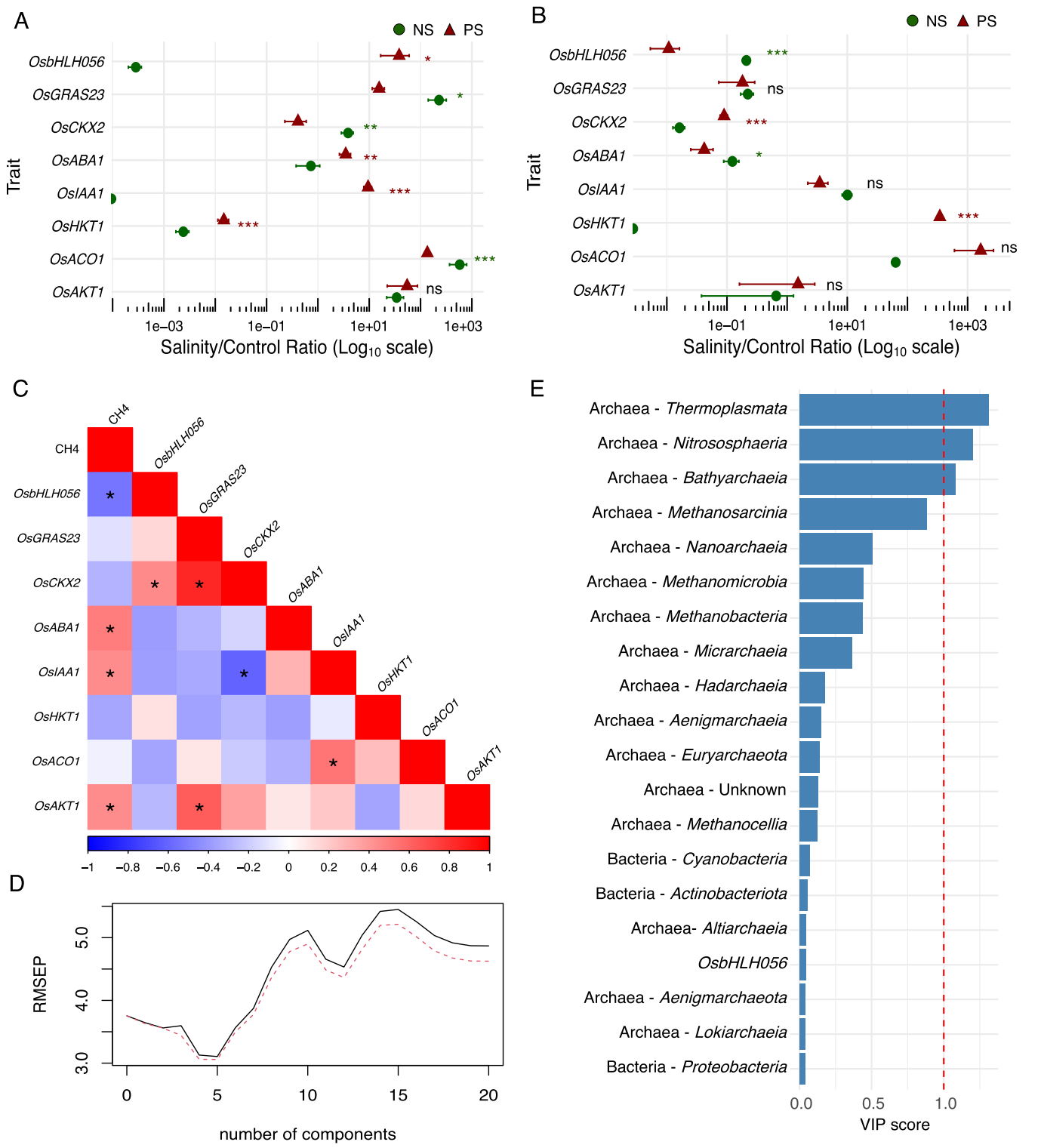

Fig. 6. Integrated statistical analyses linking gene expression, microbiome composition, and methane emissions under salinity. **(A)** Log_{10}-transformed response ratios (salinity/control) for gene expression in salt-tolerant (ST) and **(B)** salt-sensitive (SS) rice genotypes grown under nursery soil (NS, green circle) and paddy soil (PS, red triangle) conditions. **(C)** Correlation heatmap of CH_4 with stress/hormone-related genes, highlighting significant correlations. **(D)** Cross-validated root mean square error of prediction (RMSEP) curve from partial least squares regression (PLSR), indicating the optimal number of components. **(E)** Variable importance in projection (VIP) scores from the PLSR model, showing the top 20 predictors of CH_4 emissions. Archaea methanogens (e.g., Methanomicrobia, Methanobacteria) and stress-responsive genes (e.g., *OsbHLH056*, *OsABA1*, *OsAKT1*) emerged as dominant drivers. Data represent mean ± SD (n = 3). Asterisks indicate statistically significant differences between salt and control conditions for each genotype (*$P< 0.05$, **$P< 0.01$, ***$P < 0.001$; *Student's t-test*).

plants in PS exhibited higher leaf gas exchange parameters (A_n, g_s, and E), increased antioxidant enzyme activities (SOD, CAT, and APX), and greater proline accumulation, while showing lower oxidative damage markers such as malondialdehyde (MDA) and hydrogen peroxide (H_2O_2), as well as reduced Na^+ ion accumulation compared to NS-grown plants. Because NS and PS differed in both nutrient availability and microbial community composition, the superior salinity tolerance observed in PS should be interpreted as the integrated outcome of soil physicochemical properties and microbiome structure, rather than as a strictly microbiome-driven effect. Collectively, these findings suggest that soil-mediated improvements in salinity tolerance and productivity are associated with changes in the abundance and functional structure of the rhizosphere microbiome. Previous studies have shown that plant growth-promoting rhizobacteria (PGPR), including *Pseudomonas* spp., can enhance photosynthetic performance and mitigate Na^+ toxicity under saline conditions (Win et al., 2018), supporting the hypothesis that microbial interactions may contribute to stress resilience and yield stability.

To understand the contribution of the rhizobacteria to the salinity tolerance in rice, we conducted 16S rRNA sequencing and taxonomic classification analysis. Our results showed that PS had a 289% higher rhizobacterial diversity (ASVs) compared to NS, which may contribute to the enhanced salinity tolerance observed in PS-grown plants. Specific rhizobacterial composition may improve salinity tolerance (H. Li et al., 2021), particularly in salt-sensitive plant genotypes, which exhibit higher bacterial diversity (ASVs) compared to salt-tolerant plant genotypes (Lei et al., 2025). However, genotypic differences, which are related to genomic variations, may differ in root exudates and result in alterations of the rhizosphere microbiome (Aira et al., 2010). In our experiment, we found that the rhizobacteria of the SS genotype had 22% lower bacterial diversity than the ST genotype. Although ST and SS genotypes are closely related, genetic and physiological differences can influence the root exudate profile, thereby shaping distinct rhizobacterial communities. Additionally, soil stress factors such as salinity can affect the metabolic activity of the soil microbiome, hindering microbial richness, diversity, and growth (G. Zhang et al., 2023). A similar case was observed in our experiment, where an 11% reduction in the rhizobacterial diversity was noted due to 75 mM NaCl stress. When we checked the distribution of ASVs among genotypes and treatments, we found that 93% of ASVs were unique in NS, and 83% of ASVs were unique in PS.

The random forest analysis revealed that Cyanobacteria, Actinobacteria, Bacteroidia, and Bacilli were significantly shifted across all genotypes, soil types, and treatments, thereby determining microbial community divergence. These phyla are suggested to be associated with enhanced salinity tolerance in the rice, potentially contributing to plant stress adaptation. They are also the most dominant taxa in rhizosphere microbiomes (Lundberg et al., 2012), promoting plant growth through various mechanisms. Specifically, Cyanobacteria are known to be associated with photosynthesis (S. Zhang et al., 2023) and can regulate nitrogen fixation (Nawaz et al., 2024). Actinobacteria are associated with enhanced metabolite production (Hoskisson and Fernández-Martínez, 2018), Bacteroidia enhance nutrient cycling (Wang et al., 2024), and Bacilli enhance enzyme production (Danilova and Sharipova, 2020). Cyanobacteria abundance was positively correlated with plant development, whereas Actinobacteria, Bacteroidia, and *Bacilli* exhibited insignificant growth correlation. Under salinity stress, Cyanobacteria produce compounds such as phytohormones (e.g., indole-3-acetic acid), exopolysaccharides, flavonoids, and phenolic acids, which act to mitigate the harmful impacts of salt on plant physiology and structure (Ahmad et al., 2022; Harbaoui et al., 2025; Singh et al., 2011; Sodaeizadeh et al., 2025; Touzout et al., 2025). Although these observations suggest potential functional roles of these taxa, their direct contributions to plant performance and methane-related processes require experimental validation through targeted inoculation or functional omics approaches in future studies.

Rhizosphere microbiomes are assumed not only to be essential for plant growth and salinity tolerance but also to regulate carbon cycling and organic carbon inputs (Hao et al., 2022; Mosley et al., 2022; Zhao et al., 2023), which directly affect plant roots and methane emissions via methanogenic archaea in the anoxic layer of paddy soils (Rajendran et al., 2024). Due to the flooded rice cultivation practice, rice paddy fields are a significant source of CH_4 production (Lee et al., 2023; Yan et al., 2009). To determine the CH_4 emissions differences among ST and SS rice genotypes, soil types, and treatments, we recorded CH_4 production and flux. In our experiment, NS exhibited lower CH_4 emissions compared to PS; however, salinity stress significantly increased CH_4 emissions in the ST genotype. The CH_4 emissions of the SS genotype were lower than that of the ST genotype. These variations may be related to the composition of archaeal relative abundance in the rhizosphere microbiome. Furthermore, we found a significant positive correlation between CH_4 flux and the traits of *gs*, E, PRO, SOD, CAT, and APX. These results demonstrate that elevated CH_4 flux correlates with enhanced gas exchange performance and antioxidant enzyme activities in saline conditions, suggesting that methane emissions are tightly related to plant physiological traits and plant–microbe interactions, particularly with methanogenic archaea. Although soil moisture and osmotic conditions can influence methane production and diffusion in flooded paddy soils (Jäckel et al., 2001; van den Pol-van Dasselaar et al., 1998), irrigation and water management were maintained consistently across treatments in this study, minimizing confounding effects and allowing observed differences in methane emissions to be primarily attributed to salinity- and microbiome-associated biological processes.

The methanogenic archaea are primarily producers of CH_4 in the anaerobic microsites of the rice rhizosphere, where root exudates supply organic substrates for methanogenesis (Girkin et al., 2018; Ji et al., 2018; Pereira-Mora et al., 2022). The population of methanogenic archaea is positively associated with CH_4 production (Cheng et al., 2020). In our experiment, the archaeal community structure of the treatments revealed that the predominant methanogenic groups were Methanosarcina, Methanomicrobia, Methanobacteria, and Methanocellales, with their relative contributions differing according to genotype and soil type. The random forest and Pearson correlation analysis revealed that Methanobacteria and Methanocellia were the most important groups for classifying treatments, with strong positive relationships with CH_4 flux. Our results showed that these specific methanogenic taxa are strongly associated with CH_4 efflux and may contribute to methane production dynamics under salinity stress conditions, which are also known as keystone taxa contributing to CH_4 generation in paddy soils (D. Li et al., 2021).

The differing salinity tolerance observed between ST and SS genotypes grown in NS and PS soils reflects the synergistic influence of soil physicochemical properties, nutrient status, and microbial community composition (Li et al., 2020). Notably, paddy soil (PS), despite having lower nutrient content than nursery soil (NS), supported superior salinity tolerance. This suggests that high microbial diversity and specific beneficial taxa in PS may mitigate the negative effects of osmotic stress and ion antagonism—factors that often limit the efficacy of high-nutrient soils under saline conditions (Goszcz et al., 2025; Sharma et al., 2025). Because NS and PS vary in both nutrient availability and microbiome structure, their individual contributions to plant performance are deeply intertwined (Panek et al., 2026).

Root exudates are also likely to play a key role in mediating plant–microbe interactions under salinity stress (Feng, 2026; Kumar et al., 2023; Zhou et al., 2026). Plants can alter the composition and quantity of root exudates, including sugars, organic acids, amino acids, and secondary metabolites, in response to environmental conditions (Hou et al., 2026). These compounds serve as substrates and signaling molecules for rhizosphere microorganisms, potentially influencing microbial community structure and activity, including processes such as methanogenesis (Yanuka-Golub et al., 2025). Although root exudate composition was not directly quantified in this study, salinity-induced

changes in plant metabolism may have altered root exudation patterns, indirectly influencing methanogenic activity and methane emissions (Rajendran et al., 2024). This may help explain the observed differences in microbial community structure and CH_4 emissions between genotypes and soil conditions in our study. This represents a key mechanistic gap that should be addressed in future studies integrating metabolomic profiling of root exudates.

Environmental factors do not always control plant-microbe interactions but are also regulated by plant genes. Salinity stress reprogrammed stress- and hormone-related genes, and soil type affected expression patterns (Aycan, 2026; Yun et al., 2024). PS had significantly greater gene expression than NS, indicating that salinity had a lesser influence on gene activity in ST and SS genotypes. Paddy soil expressed more hormonal signaling, ion transport, and transcriptional regulatory genes (*OsABA1*, *OsCKX2*, and *OsIAA1*). However, genotype affected the ethylene biosynthesis gene *OsACO1*. This expression pattern supports the observed improvement in plant growth and salinity tolerance mediated by soil microbial communities, particularly through their influence on auxin- and ABA-related stress responses. *Trichoderma* spp. can alter root structure by increasing plant IAA levels and enhancing osmoprotectant and antioxidant activity in response to salt stress (Contreras-Cornejo et al., 2014). PGPBs can produce plant hormones like auxin (IAA), ABA, cytokinins, and gibberellins, which help regulate root growth and stress adaptation (Mishra et al., 2021). Many gene expressions were substantially linked with methane emissions. Positive associations were found between the gene expression of *OsABA1*, *OsIAA1*, and *OsAKT1* and CH_4 emissions. We discovered that salinity-induced hormonal and ion homeostasis responses may indirectly enhance methanogenesis. Although RT-qPCR was used to quantify gene expression in this study, further validation using independent biological replicates or complementary approaches (e.g., transcriptomic analyses) would strengthen the robustness and generalizability of these findings.

This study suggests that plant transcriptional responses play an important role in coordinating stress signaling, hormone regulation, and ion homeostasis under salt stress, which may influence rhizosphere microbial activity and methanogenic processes. ST grown in PS generally showed more stable gene expression profiles under salt stress. These responses were accompanied by shifts in microbial community composition linked to CH_4 production. Collectively, our results indicate that genotypes and soil types that sustain better growth and physiological activity under salt stress also exhibit higher methane emissions, highlighting a trade-off between stress tolerance and enhanced microbial methanogenesis that may be driven by plant-microbe interactions. Our results contrast with earlier reports where salinity was shown to consistently inhibit CH_4 emission. For instance, van der Gon and Neue (1995) observed a 25% reduction in CH_4 emission under salinity, primarily attributed to suppressed microbial activity. More recently, Peng et al. (2017) demonstrated that specific microbial taxonomic groups can maintain resilience under salinity stress. However, recent projections suggest that the development of salt-tolerant rice genotypes may paradoxically elevate CH_4 emissions by up to 60% through enhanced plant-mediated pathways (Anumalla et al., 2025). This aligns with our findings that physiological stability of salt-tolerant genotypes may maintain a steady substrate supply for methanogens, effectively bypassing the inhibitory effects of salinity.

From an agronomic perspective, this trade-off between enhanced salinity tolerance and increased CH_4 emissions presents a critical challenge for sustainable rice production (Ume et al., 2025). While improved plant performance under salinity stress is desirable, the associated stimulation of methanogenic activity may contribute to increased greenhouse gas emissions (Dai et al., 2023). Therefore, future strategies should aim to decouple these processes by optimizing water management practices (e.g., alternate wetting and drying), manipulating rhizosphere microbiomes through targeted inoculation or microbial engineering (Asiloglu et al., 2026), and selecting or breeding rice genotypes that maintain stress tolerance without promoting excessive carbon exudation that fuels methanogenesis (Ali et al., 2024). Integrating plant genetics with microbiome-based approaches may provide a promising pathway to balance productivity and environmental sustainability under saline conditions.

This study was conducted under controlled greenhouse conditions to elucidate mechanistic links among salinity stress, plant physiology, rhizosphere microbiomes, and methane emissions. While this approach enabled clear interpretation of microbiome-mediated responses, field-scale heterogeneity, long-term microbial succession, and seasonal environmental variability were beyond the scope of the present work. In addition, the experimental design focused on one salt-tolerant and one salt-sensitive rice genotype, allowing clear contrast of stress-response strategies but limiting broader genotype-level generalization. Root exudate composition and soil physicochemical dynamics were also not directly quantified. Additionally, key root physiological processes such as root exudation rates and root respiration were not measured in this study, which may play critical roles in shaping rhizosphere microbial activity and methane production (Yanuka-Golub et al., 2025). Despite these limitations, the observed interactions between plant physiological responses, rhizosphere microbiome composition, and methane emissions provide a useful framework for understanding similar processes under field conditions (Chukwuneme and Babalola, 2025). In natural paddy systems, spatial soil heterogeneity and seasonal shifts in microbial communities may further modulate these interactions, potentially amplifying or stabilizing the observed plant–microbe–methane relationships (Iqbal et al., 2025). Future studies incorporating diverse rice genotypes, field-based experiments, and multi-omics approaches will be important to validate and extend these findings under agronomically realistic conditions.

5. Conclusion

This study demonstrates that interactions between plants and microbiomes play an important and integrative role in shaping both salinity tolerance and CH_4 production in rice plants under salt stress conditions. Paddy soil, despite lower nutrient availability, supported a diverse microbial community that enhanced plant growth and salinity stress tolerance, likely through interactions with stress- and hormone-related transcriptional pathways. Integrated physiological traits, antioxidant activities, microbiome composition, and gene expression indicate that salinity tolerance is not regulated solely by internal plant mechanisms but emerges from synergistic interactions with rhizobacteria and methanogenic archaea. Methane emissions were closely associated with plant biomass, transcriptional regulation of stress-responsive genes, and the composition of methanogenic archaeal taxa. Together, these findings establish a mechanistic framework (Fig. 7) linking salinity tolerance, plant-microbe interactions, and methane production in rice systems, highlighting the need to balance agricultural productivity with environmental sustainability in saline paddy fields. These findings reveal a fundamental trade-off between enhanced salinity tolerance and increased CH_4 emissions, underscoring a critical challenge for climate-smart and sustainable rice production.

CRediT authorship contribution statement

Murat Aycan: Writing – review & editing, Writing – original draft, Visualization, Validation, Supervision, Resources, Project administration, Methodology, Investigation, Funding acquisition, Formal analysis, Data curation, Conceptualization. **Dorra Fakhet:** Investigation, Methodology, Data curation. **Pedro J. Picazo:** Investigation, Methodology, Data curation. **Seda Bodur:** Investigation, Data curation. **Hirohiko Nagano:** Investigation, Formal analysis. **Rasit Asiloglu:** Data curation, Formal analysis. **Iker Aranjuelo:** Supervision. **Toshiaki Mitsui:** Supervision, Funding acquisition.

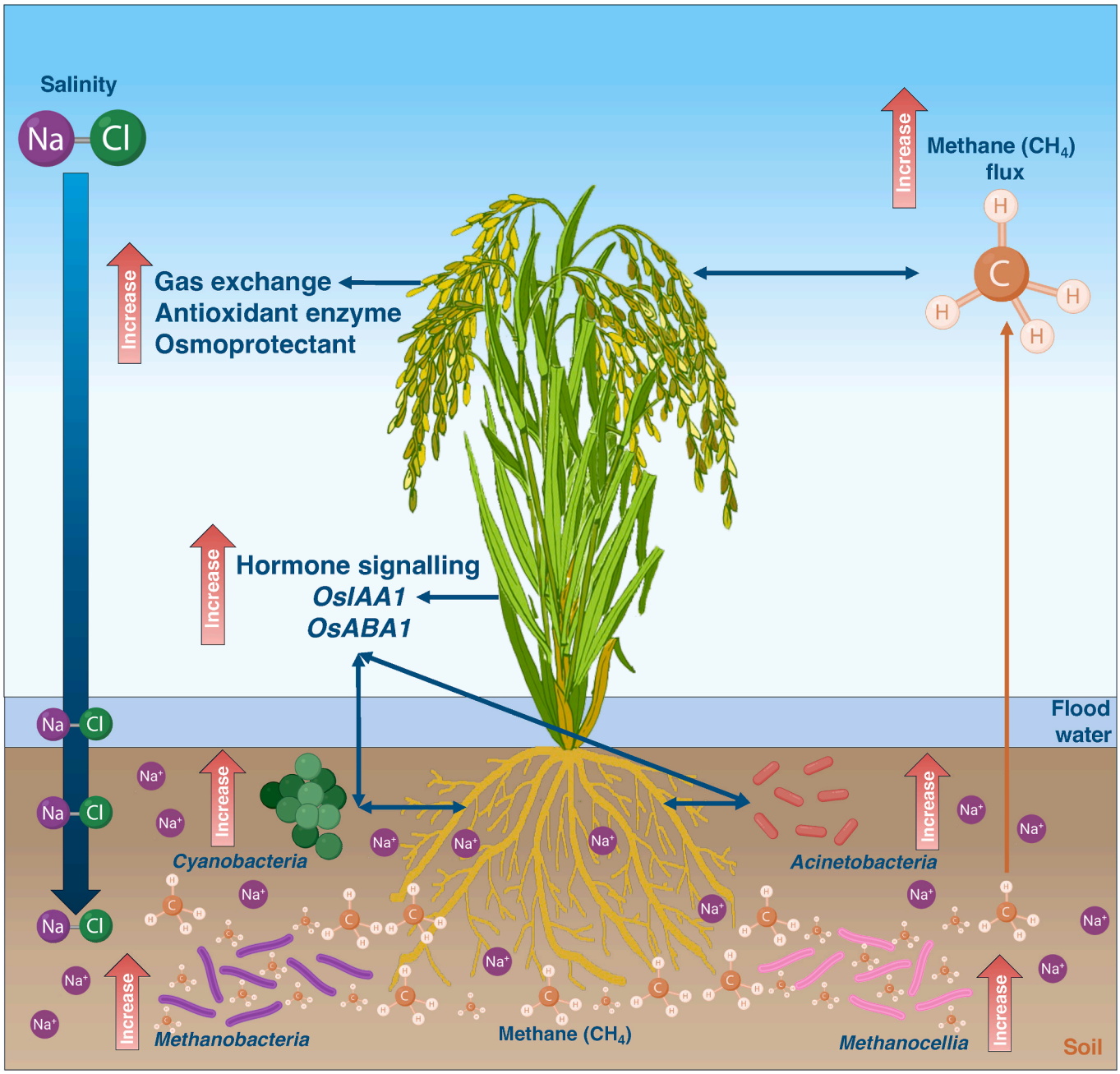

Fig. 7. Proposed mechanistic model linking plant responses, rhizosphere microbiome, and methane emissions under salinity stress. Salinity stress (Na^+/Cl^- accumulation) induces physiological and molecular adjustments in rice, including enhanced gas exchange, increased activity of antioxidant enzymes, and the accumulation of osmoprotectants. Transcriptional regulation of stress- and hormone-related genes (e.g., *OsIAA1*, *OsABA1*) supports these adaptive processes. The paddy soil microbiome further contributes to salinity tolerance: Cyanobacteria are associated with photosynthesis and nitrogen fixation, while methanogenic archaea (Methanobacteria, Methanocellia) dominate the anoxic layer, associated with increased CH_4 production. Together, plant–microbe interactions enhance growth and yield under saline conditions but concomitantly increase methane flux, highlighting a trade-off between stress adaptation and greenhouse gas emissions.

Funding

This research was funded by a Grant-in-Aid for JSPS Fellows (23KF0033) to MA; a Grant-in-Aid for Scientific Research (JP22K14804) to RA; a Grant-in-Aid for Scientific Research (24K08825); a Grant for Promotion of the "KOME Co-creation Innovation" project from Niigata University to TM; and the European Union's Horizon 2020 Research and Innovation Programme under the CropYQualT-CEC project (Grant Agreement ID: 872602).

Declaration of competing interest

The authors declare that they have no known competing financial interests or personal relationships that could have influenced the work reported in this paper.

Acknowledgments

We thank the Japan Society for the Promotion of Science for providing Murat Aycan with a Postdoctoral Fellowship for Research in Japan and the European Union's Horizon 2020 Research and Innovation

Programme under the CropYQualT-CEC project (Grant Agreement ID: 872602) for supporting Dorra Fakhet (IdAB-CSIC, Spain) and Pedro Rodriguez (IdAB-CSIC, Spain)'s research exchange in Japan.

Appendix A. Supplementary data

Supplementary data to this article can be found online at https://doi.org/10.1016/j.plaphy.2026.111324.

Data availability

Data will be made available on request.

References

Abellan-Schneyder, I., Matchado, M.S., Reitmeier, S., Sommer, A., Sewald, Z., Baumbach, J., List, M., Neuhaus, K., 2021. Primer, pipelines, parameters: issues in 16S rRNA gene sequencing. mSphere 6, 10. https://doi.org/10.1128/mSphere.01202-20.

AbuQamar, S.F., El-Saadony, M.T., Saad, A.M., Desoky, E.-S.M., Elrys, A.S., El-Mageed, T.A.A., Semida, W.M., Abdelkhalik, A., Mosa, W.F.A., Al Kafaas, S.S., Naser, S., Ibrahim, E.H., Alshamsi, F.M.K., Mathew, B.T., El-Tarabily, K.A., 2024. Halotolerant plant growth-promoting rhizobacteria improve soil fertility and plant salinity tolerance for sustainable agriculture—A review. Plant Stress 12, 100482. https://doi.org/10.1016/j.stress.2024.100482.

Aebi, H., 1984. Catalase in vitro. In: Methods in Enzymology. Academic Press, pp. 121–126. https://doi.org/10.1016/S0076-6879(84)05016-3.

Ahmad, N., Yasin, D., Bano, F., Fatma, T., 2022. Ameliorative effects of endogenous and exogenous indole-3-acetic acid on atrazine stressed paddy field cyanobacterial biofertilizer Cylindrospermum stagnale. Sci. Rep. 12, 11175. https://doi.org/10.1038/s41598-022-15415-z.

Aira, M., Gómez-Brandón, M., Lazcano, C., Bååth, E., Domínguez, J., 2010. Plant genotype strongly modifies the structure and growth of maize rhizosphere microbial communities. Soil Biol. Biochem. 42, 2276–2281. https://doi.org/10.1016/j.soilbio.2010.08.029.

Ali, Q., Ali, Mohsin, Jing, H., Hussain, A., Manghwar, H., Ali, Musrat, Raza, W., Mundra, S., 2024. Power of plant microbiome: a sustainable approach for agricultural resilience. Plant Stress 14, 100681. https://doi.org/10.1016/j.stress.2024.100681.

Amako, K., Chen, G.X., Asada, K., 1994. Separate assays specific for ascorbate peroxidase and guaiacol peroxidase and for the chloroplastic and cytosolic isozymes of ascorbate peroxidase in plants. Plant Cell Physiol. 35, 497–504. https://doi.org/10.1093/oxfordjournals.pcp.a078621.

Amaral-Zettler, L.A., McCliment, E.A., Ducklow, H.W., Huse, S.M., 2009. A method for studying protistan diversity using massively parallel sequencing of V9 hypervariable regions of small-subunit ribosomal RNA genes. PLoS One 4, e6372. https://doi.org/10.1371/journal.pone.0006372.

Anumalla, M., Catolos, M., Ramos, J., Cruz, M.T.Sta, Zhang, X., Radanielson, A., Bhosale, S., de los Reyes, B.G., Hussain, W., 2025. Salinity-tolerant rice: a sustainable solution for food security and greenhouse gas mitigation. Curr. Plant Biol. 43, 100518. https://doi.org/10.1016/j.cpb.2025.100518.

Asiloglu, R., Bodur, S.O., Samuel, S.O., Aycan, M., Murase, J., Harada, N., 2024. Trophic modulation of endophytes by rhizosphere protists. ISME J. 18, 235. https://doi.org/10.1093/ismejo/wrae235.

Asiloglu, R., Kuno, H., Fujino, M., Bodur, S., Aycan, M., Ishizuka, H., Kazama, S., Iwasaki, S., Murase, J., Harada, N., Arai, M., Ikazaki, K., 2026. Predator-mediated local convergence fosters global microbial community divergence. Nat. Commun. 17, 2499. https://doi.org/10.1038/s41467-026-70605-x.

Aycan, M., 2026. Salinity stress in rice: mechanisms and molecular approaches to mitigation. Planta 263, 82. https://doi.org/10.1007/s00425-026-04964-6.

Aycan, M., Mitsui, T., 2026. Salinity stress in rice: physiological and molecular mechanisms with a focus on the role of the *hst1* gene and *OsRR22* in enhancing salt tolerance. Crop Design 5, 100129. https://doi.org/10.1016/j.cropd.2025.100129.

Aycan, M., Mitsui, T., 2024. Regulation of common early and late stress responses in rice by transcriptional and antioxidant mechanisms under salt stress. J. Plant Growth Regul. 43, 4470–4489. https://doi.org/10.1007/s00344-024-11409-5.

Aycan, M., Nahar, L., Baslam, M., Mitsui, T., 2023. B-type response regulator *hst1* controls salinity tolerance in rice by regulating transcription factors and antioxidant mechanisms. Plant Physiol. Biochem. 196, 542–555. https://doi.org/10.1016/j.plaphy.2023.02.008.

Aycan, M., Nahar, L., Baslam, M., Mitsui, T., 2024. Transgenerationalplasticity in salinity tolerance of rice: unraveling non-geneticphenotypic modifications and environmental influences. J. Exp. Bot. 75, 5037–5053. https://doi.org/10.1093/jxb/erae211.

Bao, Q.-L., Xiao, K.-Q., Chen, Z., Yao, H.-Y., Zhu, Y.-G., 2014. Methane production and methanogenic archaeal communities in two types of paddy soil amended with different amounts of rice straw. FEMS Microbiol. Ecol. 88, 372–385. https://doi.org/10.1111/1574-6941.12305.

Bates, L.S., Waldren, R.P., Teare, I.D., 1973. Rapid determination of free proline for water-stress studies. Plant Soil 39, 205–207. https://doi.org/10.1007/BF00018060.

Bolyen, E., Rideout, J.R., Dillon, M.R., Bokulich, N.A., Abnet, C.C., Al-Ghalith, G.A., Alexander, H., Alm, E.J., Arumugam, M., Asnicar, F., Bai, Y., Bisanz, J.E., Bittinger, K., Brejnrod, A., Brislawn, C.J., Brown, C.T., Callahan, B.J., Caraballo-Rodríguez, A.M., Chase, J., Cope, E.K., Da Silva, R., Diener, C., Dorrestein, P.C., Douglas, G.M., Durall, D.M., Duvallet, C., Edwardson, C.F., Ernst, M., Estaki, M., Fouquier, J., Gauglitz, J.M., Gibbons, S.M., Gibson, D.L., Gonzalez, A., Gorlick, K., Guo, J., Hillmann, B., Holmes, S., Holste, H., Huttenhower, C., Huttley, G.A., Janssen, S., Jarmusch, A.K., Jiang, L., Kaehler, B.D., Kang, K. Bin, Keefe, C.R., Keim, P., Kelley, S.T., Knights, D., Koester, I., Kosciolek, T., Kreps, J., Langille, M.G.I., Lee, J., Ley, R., Liu, Y.-X., Loftfield, E., Lozupone, C., Maher, M., Marotz, C., Martin, B.D., McDonald, D., McIver, L.J., Melnik, A.V., Metcalf, J.L., Morgan, S.C., Morton, J.T., Naimey, A.T., Navas-Molina, J.A., Nothias, L.F., Orchanian, S.B., Pearson, T., Peoples, S.L., Petras, D., Preuss, M.L., Pruesse, E., Rasmussen, L.B., Rivers, A., Robeson, M.S., Rosenthal, P., Segata, N., Shaffer, M., Shiffer, A., Sinha, R., Song, S.J., Spear, J.R., Swafford, A.D., Thompson, L.R., Torres, P.J., Trinh, P., Tripathi, A., Turnbaugh, P.J., Ul-Hasan, S., van der Hooft, J.J.J., Vargas, F., Vázquez-Baeza, Y., Vogtmann, E., von Hippel, M., Walters, W., Wan, Y., Wang, M., Warren, J., Weber, K.C., Williamson, C.H.D., Willis, A.D., Xu, Z.Z., Zaneveld, J.R., Zhang, Y., Zhu, Q., Knight, R., Caporaso, J.G., 2019. Reproducible, interactive, scalable and extensible microbiome data science using QIIME 2. Nat. Biotechnol. 37, 852–857. https://doi.org/10.1038/s41587-019-0209-9.

Breiman, L., 2001. Random forests. Mach. Learn. 45, 5–32. https://doi.org/10.1023/A:1010933404324.

Burki, F., Roger, A.J., Brown, M.W., Simpson, A.G.B., 2020. The new tree of eukaryotes. Trends Ecol. Evol. 35, 43–55. https://doi.org/10.1016/j.tree.2019.08.008.

Cakmak, I., Marschner, H., 1992. Magnesium deficiency and high light intensity enhance activities of superoxide dismutase, ascorbate peroxidase, and glutathione reductase in bean leaves. Plant Physiol. 98, 1222–1227. https://doi.org/10.1104/pp.98.4.1222.

Callahan, B.J., McMurdie, P.J., Rosen, M.J., Han, A.W., Johnson, A.J.A., Holmes, S.P., 2016. DADA2: high-resolution sample inference from illumina amplicon data. Nat. Methods 13, 581–583. https://doi.org/10.1038/nmeth.3869.

Caporaso, J.G., Lauber, C.L., Walters, W.A., Berg-Lyons, D., Huntley, J., Fierer, N., Owens, S.M., Betley, J., Fraser, L., Bauer, M., Gormley, N., Gilbert, J.A., Smith, G., Knight, R., 2012. Ultra-high-throughput microbial community analysis on the illumina HiSeq and MiSeq platforms. ISME J. 6, 1621–1624. https://doi.org/10.1038/ismej.2012.8.

Cheng, J., Dong, H., Zhang, H., Yuan, L., Li, H., Yue, L., Hua, J., Zhou, J., 2020. Improving CH_4 production and energy conversion from CO_2 and H_2 feedstock gases with mixed methanogenic community over Fe nanoparticles. Bioresour. Technol. 314, 123799. https://doi.org/10.1016/j.biortech.2020.123799.

Chukwuneme, C.F., Babalola, O.O., 2025. Microbial diversity and function in the rhizosphere microbiome: driving forces and monitoring approaches. Agrosystems, Geosciences & Environment 8. https://doi.org/10.1002/agg2.70169.

Contreras-Cornejo, H.A., Macías-Rodríguez, L., Alfaro-Cuevas, R., López-Bucio, J., 2014. *Trichoderma* spp. improve growth of *arabidopsis* seedlings under salt stress through enhanced root development, osmolite production, and Na^+ elimination through root exudates. Mol. Plant Microbe Interact. 27, 503–514. https://doi.org/10.1094/MPMI-09-13-0265-R.

Dai, X., Sun, J., Zhao, Z., Ma, R., Zheng, Z., Liu, Y., Wang, X., Zhou, W., 2023. Linking the potential activities of methanogens and methanotrophs to their communities under different fertilization regimes in coastal saline paddy soils. Appl. Soil Ecol. 192, 105102. https://doi.org/10.1016/j.apsoil.2023.105102.

Danilova, I., Sharipova, M., 2020. The practical potential of bacilli and their enzymes for industrial production. Front. Microbiol. 11, 558639. https://doi.org/10.3389/FMICB.2020.01782/BIBTEX.

Dhindsa, R.S., Matowe, W., 1981. Drought tolerance in two mosses: correlated with enzymatic defence against lipid peroxidation. J. Exp. Bot. 32, 79–91. https://doi.org/10.1093/jxb/32.1.79.

FAO, 2009. Global agriculture towards 2050. High Level Expert Forum-How to Feed the World 2050.

Feng, J., 2026. Harnessing root-associated microbiomes to enhance plant resilience under salinity stress. Plant Cell Environ., e70442 https://doi.org/10.1111/pce.70442.

Fernández-Baca, C.P., Rivers, A.R., Kim, W., Iwata, R., McClung, A.M., Roberts, D.P., Reddy, V.R., Barnaby, J.Y., 2021. Changes in rhizosphere soil microbial communities across plant developmental stages of high and low methane emitting rice genotypes. Soil Biol. Biochem. 156, 108233. https://doi.org/10.1016/j.soilbio.2021.108233.

Flowers, T.J., Colmer, T.D., 2008. Salinity tolerance in halophytes. New Phytol. 179, 945–963. https://doi.org/10.1111/j.1469-8137.2008.02531.x.

Fukagawa, N.K., Ziska, L.H., 2019. Rice: importance for global nutrition. J. Nutr. Sci. Vitaminol. 65, S2–S3. https://doi.org/10.3177/jnsv.65.S2.

Garbeva, P., van Elsas, J.D., van Veen, J.A., 2008. Rhizosphere microbial community and its response to plant species and soil history. Plant Soil 302, 19–32. https://doi.org/10.1007/s11104-007-9432-0.

Genua-Olmedo, A., Temmerman, S., Ibáñez, C., Alcaraz, C., 2022. Evaluating adaptation options to sea level rise and benefits to agriculture: the Ebro Delta showcase. Sci. Total Environ. 806. https://doi.org/10.1016/j.scitotenv.2021.150624.

Girkin, N.T., Turner, B.L., Ostle, N., Sjögersten, S., 2018. Composition and concentration of root exudate analogues regulate greenhouse gas fluxes from tropical peat. Soil Biol. Biochem. 127, 280–285. https://doi.org/10.1016/j.soilbio.2018.09.033.

Goszcz, A., Furtak, K., Stasiuk, R., Wójtowicz, J., Musiałowski, M., Schiavon, M., Dębiec-Andrzejewska, K., 2025. Bacterial osmoprotectants—a way to survive in saline conditions and potential crop allies. FEMS Microbiol. Rev. 49. https://doi.org/10.1093/femsre/fuaf020.

Gupta, A., Singh, A.N., Tiwari, R.K., Sahu, P.K., Yadav, J., Srivastava, A.K., Kumar, S., 2023. Salinity alleviation and reduction in oxidative stress by endophytic and

rhizospheric microbes in two rice cultivars. Plants 12, 976. https://doi.org/10.3390/plants12050976.
Hao, J., Feng, Y., Wang, Xing, Yu, Q., Zhang, F., Yang, G., Ren, G., Han, X., Wang, Xiaojiao, Ren, C., 2022. Soil microbial nitrogen-cycling gene abundances in response to crop diversification: a meta-analysis. Sci. Total Environ. 838, 156621. https://doi.org/10.1016/j.scitotenv.2022.156621.
Harbaoui, A., Khelifi, N., Aissaoui, N., Muzard, M., Martinez, A., Smaali, I., 2025. A novel bioactive and functional exopolysaccharide from the cyanobacterial strain *Arthrospira maxima* cultivated under salinity stress. Bioproc. Biosyst. Eng. 48, 445–460. https://doi.org/10.1007/s00449-024-03120-2.
Henneron, L., Kardol, P., Wardle, D.A., Cros, C., Fontaine, S., 2020. Rhizosphere control of soil nitrogen cycling: a key component of plant economic strategies. New Phytol. 228, 1269–1282. https://doi.org/10.1111/nph.16760.
Hoskisson, P.A., Fernández-Martínez, L.T., 2018. Regulation of specialised metabolites in actinobacteria – expanding the paradigms. Environ. Microbiol. Rep. 10, 231–238. https://doi.org/10.1111/1758-2229.12629.
Hothorn, T., Bretz, F., Westfall, P., 2008. Simultaneous inference in general parametric models. Biom. J. 50, 346–363. https://doi.org/10.1002/bimj.200810425.
Hou, F., Hinojosa, L., Jansen, B., Morriën, E., de Vries, F.T., 2026. Plant species specific effects of root exudates on the formation and destabilization of soil organic matter. Soil Biol. Biochem. 216, 110125. https://doi.org/10.1016/j.soilbio.2026.110125.
IPCC, 2014. Climate Change 2014: Synthesis Report. Contribution of Working Groups I, II and III to the Fifth Assessment Report of the Intergovernmental Panel on Climate Change. Ipcc.
Iqbal, S., Begum, F., Nguchu, B.A., Claver, U.P., Shaw, P., 2025. The invisible architects: microbial communities and their transformative role in soil health and global climate changes. Environ. Microbiome 20, 36. https://doi.org/10.1186/s40793-025-00694-6.
Jäckel, U., Schnell, S., Conrad, R., 2001. Effect of moisture, texture and aggregate size of paddy soil on production and consumption of CH_4. Soil Biol. Biochem. 33, 965–971. https://doi.org/10.1016/S0038-0717(00)00248-0.
Ji, Y., Liu, P., Conrad, R., 2018. Change of the pathway of methane production with progressing anoxic incubation of paddy soil. Soil Biol. Biochem. 121, 177–184. https://doi.org/10.1016/j.soilbio.2018.03.014.
Kajiura, M., Tokida, T., 2021. Quantifying bubbling emission (ebullition) of methane from a rice paddy using high-time-resolution concentration data obtained during a closed-chamber measurement. J. Agric. Meteorol. 77. https://doi.org/10.2480/agrmet.D-21-00022. D-21-00022.
Kassambara, A., Mundt, F., 2016. Factoextra: Extract and Visualize the Results of Multivariate Data Analyses. CRAN. https://doi.org/10.32614/CRAN.package.factoextra. Contributed Packages.
Koc, Y.E., Aycan, M., Mitsui, T., 2024. Exogenous proline suppresses endogenous proline and proline-production genes but improves the salinity tolerance capacity of salt-sensitive rice by stimulating antioxidant mechanisms and photosynthesis. Plant Physiol. Biochem. 214, 108914. https://doi.org/10.1016/j.plaphy.2024.108914.
Kolde, R., 2010. Pheatmap: Pretty Heatmaps. CRAN. https://doi.org/10.32614/CRAN.package.pheatmap. Contributed Packages.
Kumar, N., Haldar, S., Saikia, R., 2023. Root exudation as a strategy for plants to deal with salt stress: an updated review. Environ. Exp. Bot. 216, 105518. https://doi.org/10.1016/j.envexpbot.2023.105518.
Lasar, H.G.W., Lamichhane, S., Dou, F., Gentry, T., 2025. The environmental trade-offs of applying soil amendments: microbial biomass and greenhouse gas emission dynamics in organic rice paddy soils. Appl. Soil Ecol. 208, 105977. https://doi.org/10.1016/j.apsoil.2025.105977.
Lê, S., Josse, J., Husson, F., 2008. **FactoMineR** : an *R* package for multivariate analysis. J. Stat. Software 25. https://doi.org/10.18637/jss.v025.i01.
Lee, H.J., Kim, S.Y., Kim, P.J., Madsen, E.L., Jeon, C.O., 2014. Methane emission and dynamics of methanotrophic and methanogenic communities in a flooded rice field ecosystem. FEMS Microbiol. Ecol. 88, 195–212. https://doi.org/10.1111/1574-6941.12282.
Lee, J.-H., Lee, J.-Y., Kang, Y.-G., Kim, J.-H., Oh, T.-K., 2023. Evaluating methane emissions from rice paddies: a study on the cultivar and transplanting date. Sci. Total Environ. 902, 166174. https://doi.org/10.1016/j.scitotenv.2023.166174.
Lei, J., Gu, H., Liu, Z., Hu, X., Yu, Z., Guan, Q., Jin, J., Liu, X., Wang, G., Liu, J., 2025. Recruitment of specific rhizosphere microorganisms in saline-alkali tolerant rice improves adaptation to saline-alkali stress. Sci. Total Environ. 963, 178413. https://doi.org/10.1016/j.scitotenv.2025.178413.
Li, D., Ni, H., Jiao, S., Lu, Y., Zhou, J., Sun, B., Liang, Y., 2021. Coexistence patterns of soil methanogens are closely tied to methane generation and community assembly in rice paddies. Microbiome 9, 20. https://doi.org/10.1186/s40168-020-00978-8.
Li, H., La, S., Zhang, X., Gao, L., Tian, Y., 2021. Salt-induced recruitment of specific root-associated bacterial consortium capable of enhancing plant adaptability to salt stress. ISME J. 15, 2865–2882. https://doi.org/10.1038/s41396-021-00974-2.
Li, H., Liu, L., Li, C., Liu, X., Ziadi, N., Shi, Y., 2023. Efficiency of different soil sterilization approaches and their effects on soil particle size distribution. J. Soil Sci. Plant Nutr. 23, 3979–3990. https://doi.org/10.1007/s42729-023-01315-2.
Li, J., Nie, M., Pendall, E., 2020. Soil physico-chemical properties are more important than microbial diversity and enzyme activity in controlling carbon and nitrogen stocks near Sydney, Australia. Geoderma 366, 114201. https://doi.org/10.1016/j.geoderma.2020.114201.
Liesack, W., 2000. Microbiology of flooded rice paddies. FEMS Microbiol. Rev. 24, 625–645. https://doi.org/10.1016/S0168-6445(00)00050-4.
Ling, N., Wang, T., Kuzyakov, Y., 2022. Rhizosphere bacteriome structure and functions. Nat. Commun. 13, 836. https://doi.org/10.1038/s41467-022-28448-9.
Liu, Z., Liu, J., Yu, Z., Li, Y., Hu, X., Gu, H., Li, L., Jin, J., Liu, X., Wang, G., 2022. Archaeal communities perform an important role in maintaining microbial stability under long term continuous cropping systems. Sci. Total Environ. 838, 156413. https://doi.org/10.1016/j.scitotenv.2022.156413.
Livak, K.J., Schmittgen, T.D., 2001. Analysis of relative gene expression data using real-time quantitative PCR and the $2-\Delta\Delta CT$ method. Methods 25, 402–408. https://doi.org/10.1006/METH.2001.1262.
Loreto, F., Velikova, V., 2001. Isoprene produced by leaves protects the photosynthetic apparatus against ozone damage, quenches ozone products, and reduces lipid peroxidation of cellular membranes. Plant Physiol. 127, 1781–1787. https://doi.org/10.1104/pp.010497.
Lundberg, D.S., Lebeis, S.L., Paredes, S.H., Yourstone, S., Gehring, J., Malfatti, S., Tremblay, J., Engelbrektson, A., Kunin, V., Rio, T.G. del, Edgar, R.C., Eickhorst, T., Ley, R.E., Hugenholtz, P., Tringe, S.G., Dangl, J.L., 2012. Defining the core *Arabidopsis thaliana* root microbiome. Nature 488, 86–90. https://doi.org/10.1038/nature11237.
Maier, R., Hörtnagl, L., Buchmann, N., 2022. Greenhouse gas fluxes (CO_2, N_2O and CH_4) of pea and maize during two cropping seasons: drivers, budgets, and emission factors for nitrous oxide. Sci. Total Environ. 849, 157541. https://doi.org/10.1016/j.scitotenv.2022.157541.
Mazhar, S., Pellegrini, E., Contin, M., Bravo, C., De Nobili, M., 2022. Impacts of salinization caused by sea level rise on the biological processes of coastal soils - a review. Front. Environ. Sci. 10, 909415. https://doi.org/10.3389/fenvs.2022.909415.
Minamikawa, K., Tokida, T., Sudo, S., Padre, A., Yagi, K., 2015. Guidelines for measuring CH_4 and N_2O emissions from rice paddies by a manually operated closed chamber method. National Institute for Agro-Environmental Sciences.
Mishra, P., Mishra, J., Arora, N.K., 2021. Plant growth promoting bacteria for combating salinity stress in plants – recent developments and prospects: a review. Microbiol. Res. 252, 126861. https://doi.org/10.1016/j.micres.2021.126861.
Mosley, O.E., Gios, E., Close, M., Weaver, L., Daughney, C., Handley, K.M., 2022. Nitrogen cycling and microbial cooperation in the terrestrial subsurface. ISME J. 16, 2561–2573. https://doi.org/10.1038/s41396-022-01300-0.
Munns, R., Tester, M., 2008. Mechanisms of salinity tolerance. Annu. Rev. Plant Biol. 59, 651–681. https://doi.org/10.1146/annurev.arplant.59.032607.092911.
Nahar, L., Aycan, M., Lopes Hornai, E.M., Baslam, M., Mitsui, T., 2023. Tolerance with high yield potential is provided by lower Na^+ ion accumulation and higher photosynthetic activity in tolerant YNU31-2-4 rice genotype under salinity and multiple heat and salinity stress. Plants 12, 1910. https://doi.org/10.3390/plants12091910.
Nawaz, T., Fahad, S., Saud, S., Zhou, R., Abdelsalam, N.R., Abdelhamid, M.M.A., Jaremko, M., 2024. Sustainable nitrogen solutions: cyanobacteria-powered plant biotechnology for conservation and metabolite production. Curr. Plant Biol. 40, 100399. https://doi.org/10.1016/J.CPB.2024.100399.
Ortega, T., Jiménez-López, D., Sierra, A., Ponce, R., Forja, J., 2023. Greenhouse gas assemblages (CO_2, CH_4 and N_2O) in the continental shelf of the Gulf of Cadiz (SW Iberian Peninsula). Sci. Total Environ. 898, 165474. https://doi.org/10.1016/j.scitotenv.2023.165474.
Panek, J., Gryta, A., Maj, W., Mącik, M., Oszust, K., Pertile, G., Pylak, M., Siegieda, D., Hallama, M., Hatano, R., Kandeler, E., Pathan, S.I., Pietramellara, G., Malusa, E., Weber, J., Turnau, K., Różalska, S., Frąc, M., 2026. Plant–soil–microbiome interactions: mechanisms, advances, and challenges in sustainable agriculture and healthy agroecosystems. Front. Microbiol. 17. https://doi.org/10.3389/fmicb.2026.1762743.
Peng, J., Wegner, C.-E., Liesack, W., 2017. Short-term exposure of paddy soil microbial communities to salt stress triggers different transcriptional responses of key taxonomic groups. Front. Microbiol. 8. https://doi.org/10.3389/fmicb.2017.00400 eCollection 2017.
Pequerul, A., Pérez, C., Madero, P., Val, J., Monge, E., 1993. A rapid wet digestion method for plant analysis. Optimization of Plant Nutrition 2, 3–6. https://doi.org/10.1007/978-94-017-2496-8_1.
Pereira-Mora, L., Terra, J.A., Fernández-Scavino, A., 2022. Methanogenic community linked to organic acids fermentation from root exudates are affected by rice intensification in rotational soil systems. Appl. Soil Ecol. 176, 104498. https://doi.org/10.1016/j.apsoil.2022.104498.
Quast, C., Pruesse, E., Yilmaz, P., Gerken, J., Schweer, T., Yarza, P., Peplies, J., Glöckner, F.O., 2012. The SILVA ribosomal RNA gene database project: improved data processing and web-based tools. Nucleic Acids Res. 41, D590–D596. https://doi.org/10.1093/nar/gks1219.
Radhakrishnan, N., Krishnasamy, C., 2024. Isolation and characterization of salt-stress-tolerant rhizosphere soil bacteria and their effects on plant growth-promoting properties. Sci. Rep. 14, 24909. https://doi.org/10.1038/s41598-024-75022-y.
Rajendran, S., Park, H., Kim, J., Park, S.J., Shin, D., Lee, J.-H., Song, Y.H., Paek, N.-C., Kim, C.M., 2024. Methane emission from rice fields: necessity for molecular approach for mitigation. Rice Sci. 31, 159–178. https://doi.org/10.1016/j.rsci.2023.10.003.
Rana, M.M., Takamatsu, T., Baslam, M., Kaneko, K., Itoh, K., Harada, N., Sugiyama, T., Ohnishi, T., Kinoshita, T., Takagi, H., Mitsui, T., 2019. Salt tolerance improvement in rice through efficient SNP marker-assisted selection coupled with speed-breeding. Int. J. Mol. Sci. 20, 2585. https://doi.org/10.3390/ijms20102585.
Sahu, P.K., Singh, S., Singh, U.B., Chakdar, H., Sharma, P.K., Sarma, B.K., Teli, B., Bajpai, R., Bhowmik, A., Singh, H.V., Saxena, A.K., 2021. Inter-genera colonization of *Ocimum tenuiflorum* endophytes in tomato and their complementary effects on Na^+/K^+ balance, oxidative stress regulation, and root architecture under elevated soil salinity. Front. Microbiol. 12, 744733. https://doi.org/10.3389/fmicb.2021.744733.
Sarkar, A., Kumar, P., Pramanik, K., Mitra, S., Soren, T., 2018. A halotolerant *Enterobacter* sp. displaying ACC deaminase activity promotes rice seedling growth

under salt stress. Research in Microbiologoy 169, 20–32. https://doi.org/10.1016/j.resmic.2017.08.005.
Sharma, N., Mahawar, L., Mishra, A., Albrectsen, B.R., 2025. Microbial contributions to plant growth and stress tolerance: mechanisms for sustainable plant production. Plant Stress 17, 100966. https://doi.org/10.1016/j.stress.2025.100966.
Simms, D., Cizdziel, P., Chomczynski, P., 1993. TRIzol: a new reagent for optimal single-step isolation of RNA. Focus 99–102. https://doi.org/10.1016/0003-2670(61)80041-X.
Singh, A., 2021. Soil salinization management for sustainable development: a review. J. Environ. Manag. 277, 111383. https://doi.org/10.1016/j.jenvman.2020.111383.
Singh, D.P., Prabha, R., Yandigeri, M.S., Arora, D.K., 2011. Cyanobacteria-mediated phenylpropanoids and phytohormones in rice (*Oryza sativa*) enhance plant growth and stress tolerance. Antonie Leeuwenhoek 100, 557–568. https://doi.org/10.1007/s10482-011-9611-0.
Sodaeizadeh, H., Hokmollahi, F., Ghasemi, S., Sadeghian, M., Tarrah, S., 2025. Cyanobacteria inoculation mitigates salinity stress by regulating plant growth, photosynthetic performance, elemental concentrations and yield in wheat. South Afr. J. Bot. 180, 857–869. https://doi.org/10.1016/J.SAJB.2025.04.006.
Soued, C., Bogard, M.J., Finlay, K., Bortolotti, L.E., Leavitt, P.R., Badiou, P., Knox, S.H., Jensen, S., Mueller, P., Lee, S.C., Ng, D., Wissel, B., Chan, C.N., Page, B., Kowal, P., 2024. Salinity causes widespread restriction of methane emissions from small inland waters. Nat. Commun. 15, 717. https://doi.org/10.1038/s41467-024-44715-3.
Tejera García, N.A., Olivera, M., Iribarne, C., Lluch, C., 2004. Partial purification and characterization of a non-specific acid phosphatase in leaves and root nodules of Phaseolus vulgaris. Plant Physiol. Biochem. 42, 585–591. https://doi.org/10.1016/j.plaphy.2004.04.004.
Tokida, T., 2021. Increasing measurement throughput of methane emission from rice paddies with a modified closed-chamber method. J. Agric. Meteorol. 77. https://doi.org/10.2480/agrmet.D-20-00029. D-20-00029.
Touzout, N., Ainas, M., Babaali, M., Moussa, H., Mihoub, A., Ahmad, I., Jamal, A., Danish, S., Ahmad, R., Dewir, Y.H., Székely, Á., 2025. Potential effect of non-nitrogen fixing Cyanobacteria Spirulina platensis on growth promotion of wheat (*Triticum aestivum* L.) under salt stress. Sci. Rep. 15, 29029. https://doi.org/10.1038/s41598-025-14567-y.
Ume, C., Kalu, U.F., Ezeibe, A.B.C., Ume, C.S., Ugwuoke, C.O., Onah, O., Joseph, D.C., 2025. Critical perspectives on the use of methanotrophs in rice farming: advances in microbial climate mitigation. Cleaner Food Systems 2, 100005. https://doi.org/10.1016/j.clfs.2025.100005.
van den Pol-van Dasselaar, A., van Beusichem, M.L., Oenema, O., 1998. Effects of soil moisture content and temperature on methane uptake by grasslands on sandy soils. Plant Soil 204, 213–222. https://doi.org/10.1023/A:1004371309361.
van der Gon, H.A.C.D., Neue, H.-U., 1995. Methane emission from a wetland rice field as affected by salinity. Plant Soil 170, 307–313. https://doi.org/10.1007/BF00010483.
Wang, X., Tian, W., Guan, C., Wu, X., Sun, X., Zhang, B., 2022. Global temporal evolution of CH_4 emissions via geo-economic integration. J. Environ. Manag. 305, 114377. https://doi.org/10.1016/j.jenvman.2021.114377.
Wang, Y., Sun, Q., Liu, J., Wang, L., Wu, X., Zhao, Z., Wang, N., Gao, Z., 2022. *Suaeda salsa* root-associated microorganisms could effectively improve maize growth and resistance under salt stress. Microbiol. Spectr. 10, e0134922. https://doi.org/10.1128/spectrum.01349-22.
Wang, Z., Ruan, X., Li, R., Zhang, Y., 2024. Microbial interaction patterns and nitrogen cycling regularities in lake sediments under different trophic conditions. Sci. Total Environ. 907, 167926. https://doi.org/10.1016/j.scitotenv.2023.167926.
Win, K.T., Tanaka, F., Okazaki, K., Ohwaki, Y., 2018. The ACC deaminase expressing endophyte *Pseudomonas* spp. enhances NaCl stress tolerance by reducing stress-related ethylene production, resulting in improved growth, photosynthetic performance, and ionic balance in tomato plants. Plant Physiol. Biochem. 127, 599–607. https://doi.org/10.1016/j.plaphy.2018.04.038.
Xavier, J.F., Costa, D.P. da, Gonçalves, J.V. da S., Pinto, M.C.F., Goulart, R.S., Zonta, E., Coelho, I. da S., 2024. Different halophytes orchestrate microbial diversity in the rhizosphere of salinity-impacted soils. Appl. Soil Ecol. 202, 105588. https://doi.org/10.1016/j.apsoil.2024.105588.
Xun, W., Liu, Y., Ma, A., Yan, H., Miao, Y., Shao, J., Zhang, N., Xu, Z., Shen, Q., Zhang, R., 2024. Dissection of rhizosphere microbiome and exploiting strategies for sustainable agriculture. New Phytol. 242, 2401–2410. https://doi.org/10.1111/nph.19697.
Yan, X., Akiyama, H., Yagi, K., Akimoto, H., 2009. Global estimations of the inventory and mitigation potential of methane emissions from rice cultivation conducted using the 2006 intergovernmental panel on climate change guidelines. Glob. Biogeochem. Cycles 23. https://doi.org/10.1029/2008GB003299.
Yanuka-Golub, K., Korenblum, E., Aronson, E.L., Matzrafi, M., 2025. Linking microbial-mediated methane production in wetlands to invasive plants. Soil Biol. Biochem. 210, 109944. https://doi.org/10.1016/j.soilbio.2025.109944.
Yilmaz, P., Parfrey, L.W., Yarza, P., Gerken, J., Pruesse, E., Quast, C., Schweer, T., Peplies, J., Ludwig, W., Glöckner, F.O., 2014. The SILVA and "All-species Living Tree Project (LTP)" taxonomic frameworks. Nucleic Acids Res. 42, D643–D648. https://doi.org/10.1093/nar/gkt1209.
Yun, P., Kaya, C., Shabala, S., 2024. Hormonal and epigenetic regulation of root responses to salinity stress. Crop J. 12, 1309–1320. https://doi.org/10.1016/j.cj.2024.02.007.
Zhang, G., Bai, J., Jia, J., Wang, W., Wang, D., Zhao, Q., Wang, C., Chen, G., 2023. Soil microbial communities regulate the threshold effect of salinity stress on SOM decomposition in coastal salt marshes. Fundam. Res. 3, 868–879. https://doi.org/10.1016/j.fmre.2023.02.024.
Zhang, G., Bai, J., Zhai, Y., Jia, J., Zhao, Q., Wang, W., Hu, X., 2024. Microbial diversity and functions in saline soils: a review from a biogeochemical perspective. J. Adv. Res. 59, 129–140. https://doi.org/10.1016/j.jare.2023.06.015.
Zhang, S., Sun, J., Feng, D., Sun, H., Cui, J., Zeng, X., Wu, Y., Luan, G., Lu, X., 2023. Unlocking the potentials of cyanobacterial photosynthesis for directly converting carbon dioxide into glucose. Nat. Commun. 14, 3425. https://doi.org/10.1038/s41467-023-39222-w.
Zhao, M., Zhao, Y., Gao, W., Xie, L., Zhang, G., Song, C., Wei, Z., 2023. Exploring the nitrogen fixing strategy of bacterial communities in nitrogen cycling by adding calcium superphosphate at various periods during composting. Sci. Total Environ. 901, 166492. https://doi.org/10.1016/j.scitotenv.2023.166492.
Zhao, Q., Jia, J., Song, F., Li, T., Zhang, W., Huang, Y., 2025. Variations in the archaeal community in wetlands soils under various hydrologic conditions in the yellow river Estuary. Front. Mar. Sci. 12, 1564173. https://doi.org/10.3389/fmars.2025.1564173.
Zhou, L., Zhu, X., Fu, Y., Luo, W., Leng, F., Wang, Y., Yang, H., Li, S., Wang, X., 2026. The mechanisms of interaction between alfalfa root exudates and rhizosphere bacterial communities for adaptation to salt stress. Environ. Exp. Bot. 244, 106344. https://doi.org/10.1016/j.envexpbot.2026.106344.